Reclaiming freshwater sustainability in the Cadillac Desert

John L. Sabo[a,1], Tushar Sinha[a,2], Laura C. Bowling[b], Gerrit H. W. Schoups[c], Wesley W. Wallender[d,e], Michael E. Campana[f], Keith A. Cherkauer[g], Pam L. Fuller[h], William L. Graf[i], Jan W. Hopmans[d], John S. Kominoski[j,3], Carissa Taylor[k], Stanley W. Trimble[l], Robert H. Webb[m], and Ellen E. Wohl[n]

[a]*Faculty of Ecology, Evolution and Environmental Sciences, School of Life Sciences, Arizona State University, PO Box 874501, Tempe, Arizona, 85287-4501;* [b]*Department of Agronomy, Purdue University, West Lafayette, IN 47907-2054;* [c]*Department of Water Resources Management, Delft University of Technology, 2600 GA, Delft, The Netherlands;* [d]*Department of Land, Air and Water Resources, University of California, Davis, CA 95616-8628;* [e]*Department of Biological and Agricultural Engineering, University of California, Davis, CA 95616-8628;* [f]*Department of Geosciences, Oregon State University, Corvallis, OR 97331-5506;* [g]*Department of Agricultural and Biological Engineering, Purdue University, West Lafayette, IN 47907-2093;* [h]*US Geological Survey, Southeast Ecological Science Center, Gainesville, FL 32653;* [i]*Department of Geography, University of South Carolina, Columbia, SC 29208;* [j]*Department of Forest Sciences, University of British Columbia, Vancouver, BC, Canada V6T 1Z4;* [k]*School of Sustainability, Arizona State University, Tempe, AZ 85287-5502;* [l]*Department of Geography, University of California, Los Angeles, CA 90095;* [m]*US Geological Survey, Tucson, AZ 85719; and* [n]*Department of Geosciences, Warner College of Natural Resources, Fort Collins, CO 80523-1482*

Edited by Glen M. MacDonald, University of California, Los Angeles, CA, and accepted by the Editorial Board November 10, 2010 (received for review July 6, 2010)

Increasing human appropriation of freshwater resources presents a tangible limit to the sustainability of cities, agriculture, and ecosystems in the western United States. Marc Reisner tackles this theme in his 1986 classic *Cadillac Desert: The American West and Its Disappearing Water*. Reisner's analysis paints a portrait of region-wide hydrologic dysfunction in the western United States, suggesting that the storage capacity of reservoirs will be impaired by sediment infilling, croplands will be rendered infertile by salt, and water scarcity will pit growing desert cities against agribusiness in the face of dwindling water resources. Here we evaluate these claims using the best available data and scientific tools. Our analysis provides strong scientific support for many of Reisner's claims, except the notion that reservoir storage is imminently threatened by sediment. More broadly, we estimate that the equivalent of nearly 76% of streamflow in the Cadillac Desert region is currently appropriated by humans, and this figure could rise to nearly 86% under a doubling of the region's population. Thus, Reisner's incisive journalism led him to the same conclusions as those rendered by copious data, modern scientific tools, and the application of a more genuine scientific method. We close with a prospectus for reclaiming freshwater sustainability in the Cadillac Desert, including a suite of recommendations for reducing region-wide human appropriation of streamflow to a target level of 60%.

Manifest Destiny and the westward expansion of European civilization in the United States during the 19th century were predicated on an adequate freshwater supply. The assumption of adequate freshwater in the western United States was justified by the prevailing view of hydroclimate, which included a theory that agriculture would stimulate rainfall, or "rain would follow the plow." Early stewards of freshwater resources—like John Wesley Powell—warned that the American West was a desert, only a small fraction of which could be sustainably reclaimed (1).* Notably, Powell remarked that irrigation would be required in the arid region west of the 100th meridian, to make the parcels provided by the Homesteading Act livable (3). Indeed, irrigation was necessary to create a sustainable society in the western United States. Today dams, irrigated agriculture, and large cities are the hallmark of western US landscapes. There are more than 75,000 dams in the United States, and the largest five reservoirs by storage capacity lie west of the 100th meridian. The storage capacity of US reservoirs increased steadily between 1950 and 1980—from 246 to 987 km^3 (4)—and the beginning of these "go-go years" of dam building (5) coincides with the US "baby boom" (roughly 1943–1964). Since that time, there has been an exodus from east to west: population of the 15 largest eastern US cities has declined by an average of 51% but increased by 32% in western cities (6, 7). Similarly, although 74% of the cropland in the coterminous United States lies in the eastern United States, 68–75% of the revenue from vegetables, fruits, and nuts derives from western farms (8). Water—not rain—has followed the plow, exceeding the expectations of even the most zealous proponents of Manifest Destiny 150 y ago.

Reisner and the Cadillac Desert

Numerous critiques of the sustainability of freshwater infrastructure in the western United States have appeared (5, 9–12). Most poignant of these is Marc Reisner's book *Cadillac Desert: The American West and Its Disappearing Water*. Reisner sketches a portrait of the political folly of western water projects; his principal argument is that impaired function of dams, reservoirs, and crop lands, coupled with rapidly growing western cities, would eventually pit municipal water users against farms and catalyze an apocalyptic collapse of western US

Author contributions: J.L.S., L.C.B., and E.E.W. designed research; J.L.S., T.S., L.C.B., G.H.W.S., W.W.W., K.A.C., W.L.G., J.S.K., C.T., S.W.T., and E.E.W. performed research; J.L.S., T.S., L.C.B., G.H.W.S., W.W.W., and P.L.F. analyzed data; J.L.S., T.S., L.C.B., G.H.W.S., W.W.W., M.E.C., P.L.F., W.L.G., J.W.H., J.S.K., C.T., S.W.T., R.H.W., and E.E.W. wrote the paper; and T.S. coded, calibrated, and implemented hydrologic models.

The authors declare no conflict of interest.

This article is a PNAS Direct Submission. G.M.M. is a guest editor invited by the Editorial Board.

[1]To whom correspondence should be addressed. E-mail: john.l.sabo@asu.edu.

[2]Present address: Department of Civil, Construction, and Environmental Engineering, North Carolina State University, Raleigh, NC 27695-7908.

[3]Present address: Odum School of Ecology, University of Georgia, Athens, GA 30602.

This article contains supporting information online at www.pnas.org/lookup/suppl/doi:10.1073/pnas.1009734108/-/DCSupplemental.

*Powell writes: "A rough estimate may be made that [404,686 square kilometers] can be redeemed at the rate of [$2,470 per square kilometer] that is for US $1 billion [in 1890]. In this work vast engineering enterprises must be undertaken. To take water from streams and pour them upon the lands, diverting dams must be constructed and canals dug." The area of irrigated croplands as of 2000 is 173,858 square kilometers, as referenced in: de Buys (2).

society.[†] In this article we explore some of the trends described by Reisner more than 2 decades ago using a more up to date and scientific approach. Specifically, we compare hypothetical calamity in the West with a control by means of direct comparison with watersheds east of the 100th meridian. The 100th meridian has some historical importance because it was the line implicated by Powell—and advocated by Reisner—as a dividing line between climates capable of supporting rainfed agriculture and regions where irrigation was necessary for dependable harvest. For the remainder of this article we use the 100th meridian as the dividing line between east and west regions in the coterminous United States. Thus, we explore whether the problems Reisner envisioned in *Cadillac Desert* exist and are unique to western watersheds. More importantly, we present a suite of metrics and indicators that summarize freshwater sustainability (or departures from sustainability) in the Cadillac Desert region.

We first synthesize a comprehensive geographic dataset that allows us to quantify and compare regional patterns of freshwater sustainability east and west of the 100th meridian. In doing this we combine data from humid western basins (i.e., Columbia) with those in more arid western regions (i.e., Colorado) for much of our analysis, noting important exceptions where necessary. Inclusion of the Columbia River basin was necessary for two reasons. First, the Columbia basin is a prime example of the grand scale of water projects that characterize development of the western United States. Second, the Columbia River originates in part in the Snake River headwaters on the Columbia Plateau, a semiarid region that illustrates many of the same impacts associated with large-scale water projects as outlined in *Cadillac Desert*. We define freshwater sustainability as renewable surface water—hereafter "streamflow"—and its allocation to people, farms, and ecosystems. We exclude groundwater as a source of freshwater in our analysis because it is not as immediately renewable as surface water, and it is less relevant to our objective because Reisner's focus was on harnessing surface water. Below we quantify patterns of mean annual streamflow in the coterminous United States. We then quantify freshwater sustainability in terms of (*i*) human water stress, (*ii*) the efficacy and lifespan of reservoir storage, (*iii*) the impact of salt loads in croplands on agricultural revenue, and (*iv*) biodiversity and invasion of native fish faunas. After analyzing broad patterns of sustainability and comparing sustainability indices east and west of the 100th meridian, we narrow our focus to the arid lands west of this divide and estimate water stress to assess the future for sustainable urban growth in the region.

Results

Climate and Surface Water Supply Set the Stage. One of Powell's key observations was that rainfall was insufficient to provide adequate vadose zone water storage during the growing season for nonirrigated agriculture in much of the western United States. The upshot of this observation was that streamflow would need to be harnessed to provide irrigation and sustain agriculture. Estimated streamflow normalized by area (runoff) is low (<10 cm) for most of the west and much higher (≥40–100 cm) for much of the eastern United States (Fig. 1*A*), with two notable exceptions. First, the Pacific Northwest and the northern mountains of California have the highest runoff in the coterminous United States. Second, the longitude of the east–west transition between high and low runoff in the Great Plains varies by nearly 10°—from the 95th meridian in the northern plains to the 105th meridian near the Gulf of Mexico. However, there are clear differences in the distribution of runoff, cities, and farms in eastern and western US watersheds. Below we define US watersheds using boundaries of the US Geological Survey (USGS) four-digit hydrologic unit code regions or hydrologic subregions (13). Cities and farms are more likely found in hydrologic subregions with abundant surface water (runoff >40 cm) in the East (nearly 94% of the population and 65% of the cropland in the East is in a hydrologic subregion with streamflow exceeding 40 cm, compared with 55% of the population and 41% of the croplands in the West). More relevant to the thesis of *Cadillac Desert*, 23% of the population and 28% of the cropland in the West falls within a hydrologic subregion where runoff is <10 cm [compared with 1% and 13% of the population and cropland, respectively, found in a hydrologic subregion with similarly low (10 cm) mean annual streamflow east of the 100th meridian].

State of Current Infrastructure. The impacts of dams and reservoirs include increases in hydrologic storage and fragmentation of river networks. Relative storage capacity gives a measure of the number of years of average streamflow stored in the reservoir system, and dam density provides a proxy for fragmentation of river networks by impoundments. Total storage capacity of reservoirs does not differ east and west of the 100th meridian (Fig. S1). Storage in more numerous but smaller reservoirs in the East is nearly equivalent to that in the generally fewer, larger reservoirs in the West. As a result, dam density is higher in the eastern United States (Figs. 1*B* and 2*A*). However, more than 73% of watersheds with relative storage capacity values >1 are located in the West, and another 19% straddle the 100th meridian between −90° to −100° W. Overall, relative storage

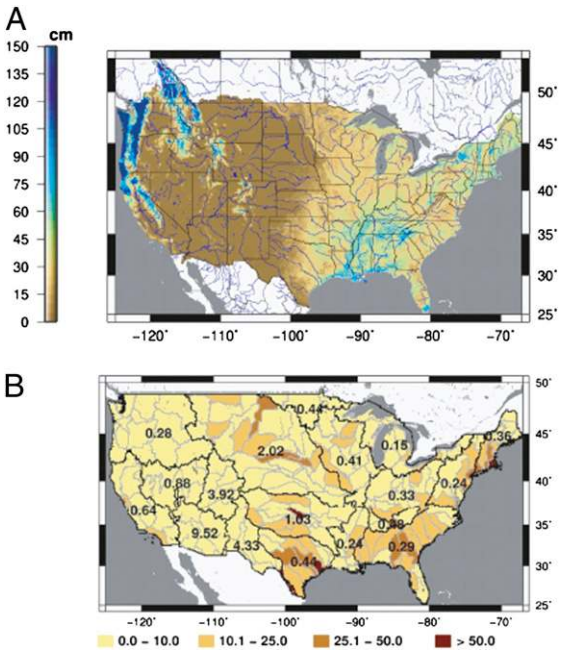

Fig. 1. Patterns of hydroclimate and freshwater infrastructure in the coterminous United States. (*A*) Mean annual streamflow (cm) estimated using the VIC macroscale hydrologic model (*SI Appendix*). (*B*) Average number of dams per 100 km of river length (color coded, see legend) in each USGS hydrologic subregion in the coterminous United States and total storage capacity per unit streamflow, or *relative* storage capacity (text) for each USGS hydrologic region.

[†]The apocalypses sketched by Reisner in *Cadillac Desert* are (*i*) that western reservoirs will fill with sediment soon, and reduced storage capacity will present unprecedented water scarcity issues; (*ii*) crop lands will be increasingly retired due to salinity issues, to the extent that water projects will ultimately poison the farmlands that western societies depend on for food; and (*iii*) growing urban populations will draw increasing water away from agricultural areas, further reducing the capacity for the West to feed its people.

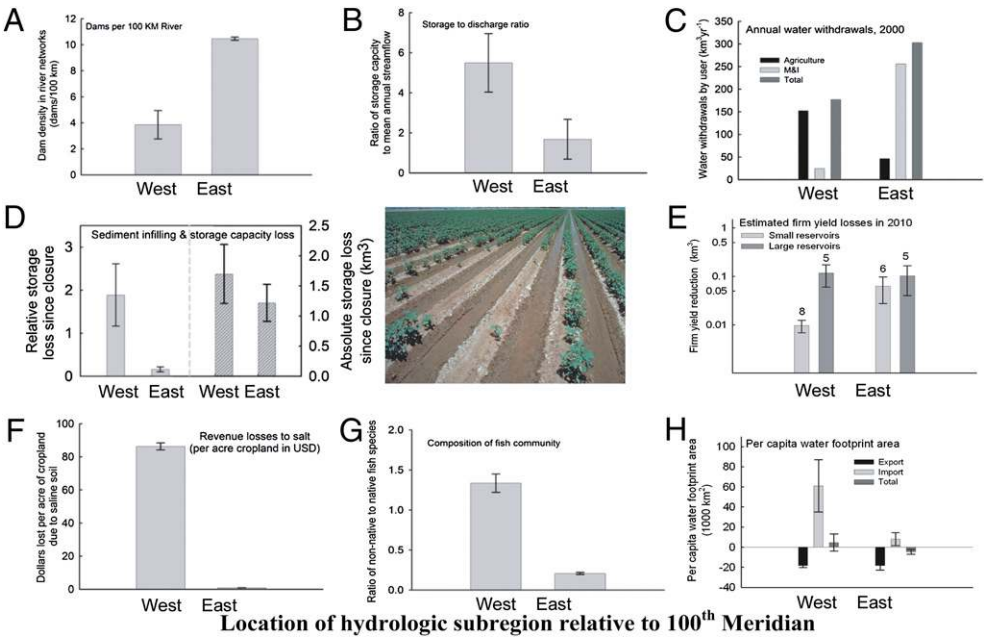

Fig. 2. Comparison of infrastructure and impacts of infrastructure east and west of the 100th meridian. (*A*) Average number of dams per 100 km of river length. (*B*) Relative storage capacity (total reservoir storage/mean annual streamflow). (*C*) Sum of water withdrawals by category—municipal, industrial, agricultural, and total. (*D*) Average storage capacity losses in reservoirs as a result of sediment infilling expressed relative to mean annual streamflow (*Left*) and in absolute terms (km^3, *Right*). (*E*) Estimated average reductions in firm yield (km^3) for large (>1.23 km^3) and small (<1.23 km^3) reservoirs. Numbers above error bars (±1 SE) are sample sizes in each category. (*F*) Estimated average revenue losses (millions USD) as a result of salt accumulation in croplands. (*G*) Average ratio of nonnative to native fishes (color) and number of nonnative species (text). (*H*) Average per capita virtual water footprints (VWF) for all metropolitan statistical areas >100,000 in size. Footprints are negative if virtual water is exported in crops from the watershed hosting the city, or positive if the city requires imports of virtual water (in crops) to feed the population. Error bars are SEs using hydrologic subregions as the unit of replication (127 and 77 east and west of the 100th meridian, respectively), unless otherwise indicated.

is 3.3 times higher in the West (Figs. 1*B* and 2*B*). Dams fragment riverscapes more in the East, but large reservoirs alter hydrologic dynamics more in the West—holding more water relative to streamflow.

Focus Area 1: Human Water Stress. Total annual water withdrawals are 1.7-fold higher in the East, but the withdrawals for agriculture are 3.2-fold higher in the West (Fig. 2*C*). To assess the sustainability of surface water withdrawals in the United States, we estimated the water scarcity index (WSI) (14, 15) for each hydrologic subregion. WSI is the ratio of total withdrawals of freshwater for human use (W) (16) to renewable supply (mean annual streamflow, MAF). We defined supply as the sum of local and unused upstream annual average streamflow estimated by the variable infiltration capacity (VIC) model (*SI Appendix*). Our application of WSI provides a measure of freshwater sustainability defined as the capacity for locally generated and unused upstream streamflow to meet local demand. Subregions with WSI ≈0 appropriate little of their streamflow. Higher WSI indicates greater appropriation of local renewable freshwater resources. WSI values >1 are possible where streamflow is low and withdrawals include a substantial groundwater component. Water stress is commonly defined as WSI 0.4 (14), indicating 40% appropriation of renewable fresh water resources. This threshold is set at less than half of available streamflow to buffer against high spatial and temporal variability in streamflow and to set aside water for ecosystems, navigation, and recreation. Water stress occurs in 58% of subregions in the West, compared with 10% in the East (Fig. 3*A*), and withdrawals exceed local streamflow by 2-fold (WSI >2) in 10 western watersheds. Nine of the top 10 WSI values are in the West (Fig. 3*A*; average ± SE WSI: 0.85 ± 0.1 West and 0.22 ± 0.03 East). In a few eastern subregions WSI is high because withdrawals from large freshwater lakes (e.g., the Laurentian Great Lakes) in neighboring subregions exceed local streamflow. Finally, consumptive use values were not estimated in 2000, such that our estimates of WSI include consumptive and nonconsumptive withdrawals of freshwater (*SI Appendix*).

Focus Area 2: Efficacy and Lifespan of Reservoir Storage. One of Reisner's key criticisms of western reliance on reservoir storage was inevitable sediment infilling and subsequent storage deficits for growing cities and agriculture (17).[‡] The question we ask here is not whether, but how fast will the nation's reservoirs fill with sediment? Assuming observed infilling rates over the last century are representative and constant, we estimate that 276 of the reservoirs (22%) in the Reservoir Sedimentation Survey Information System (RESIS-II) are already completely filled with sediment or have been dredged to maintain function. However, only 1 of these reservoirs is >0.123 km^3 (moderately sized), and only 11 are even within an order of magnitude of this size (2 in the West and 9 in the East >0.0123 km^3; Fig. S2). Predicted minimum lifespans for the remaining (unfilled) reservoirs are lowest in the central United States and Desert Southwest (Fig. S2); however, estimated minimum lifespans are all ≥1.5–2 centuries. Thus, although Reisner was correct that reservoirs fill with sediment, observed infilling and complete loss of storage function is by no means exclusively a western phenomenon and will not likely occur for most large reservoirs in the foreseeable future. Given the long time horizon for complete infilling, we extrapolated estimated capacity losses from single structures to entire hydrologic subregions to construct a metric of storage loss more comparable to available water supply. We normalized this estimate of regional storage loss by MAF because this metric better quantifies the change in the region's ability to withstand prolonged drought or flooding (15). Relative capacity losses for the 95 (of 204) subregions with adequate data from RESIS-II range from 8×10^{-4} to >11 (units = mean annual streamflow equivalents) and are higher by a factor of ≈11.7 in the West (Figs. 2*D* and 3*B*).

Storage loss in a water supply reservoir directly impacts the firm yield, or the largest withdrawal rate that the reservoir can reliably provide. The relationship between firm yield and active storage is generally nonlinear, with an initially

[‡]In the second printing of *Cadillac Desert*, Reisner writes (p 473), "As a result of [intensive machine based agriculture and loopholes allowing for agriculture on Class VI land]—and because it was inevitable anyway—the dams are silting up." He then lists infilling statistics for 12 reservoirs in the United States, including Lake Mead, writing (p 474), "In thirty five years, Lake Mead was filled with more acre feet of silt than 98% of the reservoirs in the United States are filling with acre feet of water. The rate has slowed considerably since 1963, because the silt is now building up behind Flaming Gorge, Blue Mesa and Glen Canyon dams."

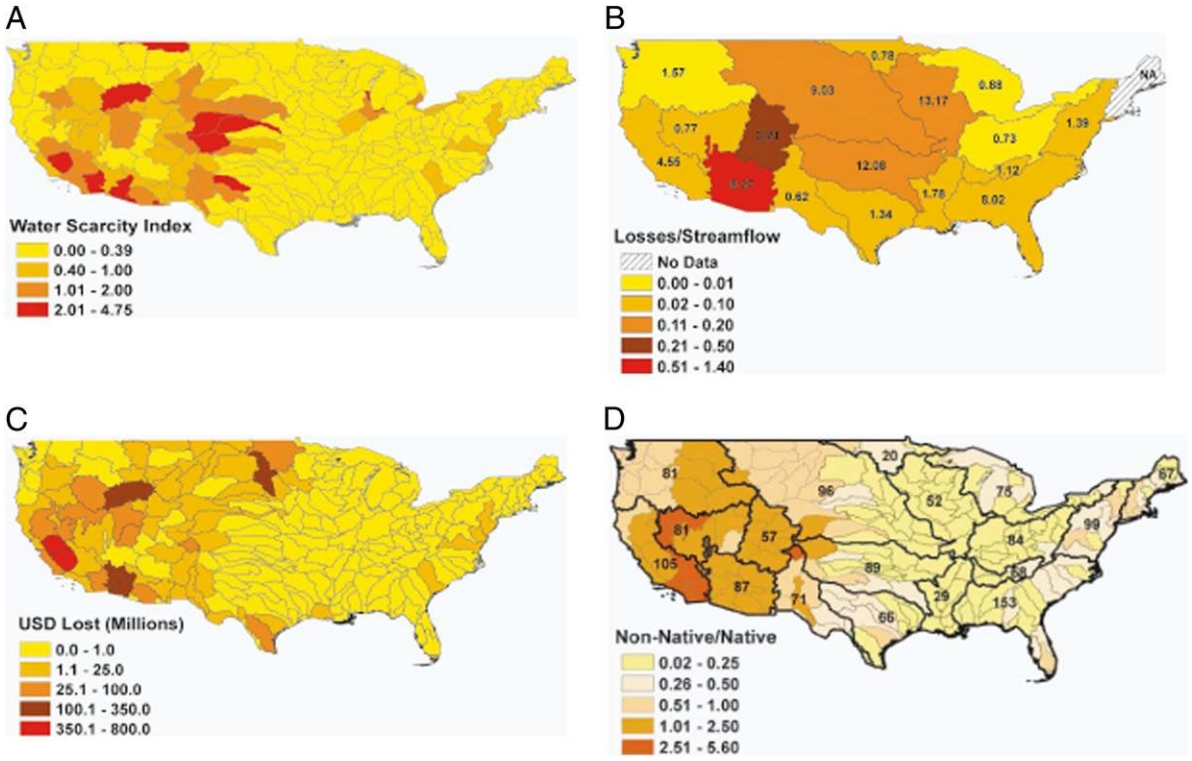

Fig. 3. Assessment of current freshwater sustainability. (*A*) WSI for 204 coterminous hydrologic subregions. Here, WSI = W/MAF, where W is total withdrawals based on USGS estimates from 2000, and MAF is total mean annual streamflow, including locally generated streamflow and flow unused by upstream hydrologic regions. (*B*) Estimated relative (storage loss/streamflow, color coded) and total losses (km^3, text) of storage capacity in each USGS hydrologic region due to infilling by sediment. NA in Hydrologic Region 1 indicates no sediment surveys available for reservoirs over 1.23×10^{-2} km^3 in this region (*SI Appendix*). (*C*) Agricultural revenue lost (in million USD) at HUC 4 scale due to soil salinization (color coded). (*D*) Ratio of nonnative to native fish species (color coded) and total number of observed nonnative species (text).

shallow—but accelerating—rate of decline in firm yield as active storage capacity decreases (Fig. S2). Firm yield for large reservoirs (>1.2 km^3, storage capacity) has already diminished by ≈1.9% relative to yield at original capacity, and up to 6.25% for small reservoirs (1.2 km^3 > storage capacity > 0.12 km^3). The absolute decline in firm yield since dam closure was not significantly different in the East and West for the reservoirs we analyzed (Table S1) except for small reservoirs, in which decline in absolute firm yield was marginally higher in the East (Fig. 2*E*). Although the differences in sediment related reductions in firm yield across the country were not generally significant in eastern relative to western reservoirs, estimated reductions in the absolute volume of firm yield losses in the West even for the small number of structures analyzed here are formidable. Estimated reductions in firm yield in the five large reservoirs we analyzed west of the 100th meridian (firm yield volume ≈0.584 $km^3 \cdot y^{-1}$) are larger in sum than maximum annual conveyance by the Los Angeles Aqueduct (≈0.25 $km^3 \cdot y^{-1}$) and Moffat Tunnel diversion to Denver (≈0.43 $km^3 \cdot y^{-1}$), and equivalent to 60% and 32% of the annual conveyance of the Salt River Project (≈0.97 $km^3 \cdot y^{-1}$) and Central Arizona Phoenix Project (≈1.85 $km^3 \cdot y^{-1}$), respectively.

Focus Area 3: Impact of Salt Loads in Croplands on Agricultural Revenue. Salinity is a worldwide threat to the sustainability of irrigated agriculture (17). Both the accumulation of salt and the extent of salt-affected soils are more prevalent in the West (Fig. 3*C* and Fig. S3). Total estimated revenue losses experienced by the agricultural sector are ≈2.8 billion US dollars (USD) annually. Estimated revenue losses are nearly an order of magnitude higher in the West (2.55 billion USD $\cdot y^{-1}$, West vs. 267 million USD $\cdot y^{-1}$, East). Crop yields and revenue have been disproportionately affected in western watersheds, particularly in regions with extensive areas of vegetable crops and orchards (Fig. 3*C*). Revenue losses are ≈60-fold higher per acre of cropland in the West (Fig. 2*F*).

Focus Area 4: Biodiversity and Invasion of Native Fish Faunas. The sustainability of fresh water supplies can be measured in terms of human water security and the capacity of freshwater ecosystems to support biodiversity (18). These two sustainability goals are not mutually exclusive—biodiversity provides valuable ecosystem services ranging from the food and economic benefits of inland fisheries (19) to the maintenance of water quality (20) and regulation of gas exchange between freshwater ecosystems and the atmosphere (21). Discharge magnitude and variation determine biodiversity in rivers across the globe (e.g., refs. 22 and 23), and dams, water diversions, and human appropriation of streamflow homogenize this variation (24), thereby altering key components of biodiversity, including food chain length (25) and the number of nonnative species, especially fishes (26, 27).

The proportion of all species that are nonnative provides a proxy for the impact of freshwater infrastructure on native biodiversity because dams and reservoirs facilitate invasion by nonnative fishes by creating new habitat (e.g., still reservoirs rather than flowing water) and altering the flow and temperature regime in dam "tailwaters" (26, 28, 29). Further, this ratio is one of four drivers used in broad-scale analyses of threats to human water security and biodiversity (18, 30). This ratio is higher in the West (Figs. 2*G* and 3*D*), and this is not a byproduct of higher native species richness in the East, because the absolute number of nonnative species is also higher (Fig. S4). Thus, dominance of

western fish faunas by nonnative fishes results from higher absolute numbers of established nonnative fishes and low species richness of native fishes (Fig. 2*G*). Moreover, of the 25 most widespread nonnative fishes west of the Mississippi River drainage,[§] 56% (14 of 25) are piscivores native to lakes or rivers in hydrologic regions east of the 100th meridian with a less variable hydrologic regime, and 6 of these 25 are capable of eating not only native insectivores but also nonnative piscivores on the basis of body and gape size (Table S2). Eastern faunas not only dominate the species roster in western rivers, but they likely occupy one or more unique trophic levels at the apex of food webs in heavily modified western rivers. This artificial increase in food chain length is due in part to a reduction in discharge variability below dams (24, 25).

Civilization, If You Can Keep It. The central theme of *Cadillac Desert* is that the hydroclimate of the American West is not generous enough to sustain cities and agriculture, especially in the Southwest. Below we attempt to quantify this claim in two ways. First, we estimate agricultural water footprints of all large (>100,000 in size) US metropolitan statistical areas (MSAs) in the East and West. Our water footprints explicitly consider the net transfer of virtual water needed to feed the local population. Second, we estimate the total appropriation of surface water by humans for a seven-region area constituting the Desert Southwest. We estimate human appropriation of surface water for this "superregion" under all possible combinations of the following scenarios: using current withdrawals (as in Fig. 3*A* but at a larger resolution) or total water demand including the virtual water required for food production; and using Census 2000 population estimates, or assuming a doubling of the Census 2000 population.

Disproportionately large water footprints of cities in the US Southwest. Agricultural water footprints are the volume of water needed to meet the food demand for a city or region (31). Here, we normalize the water volume by runoff to find the equivalent land area to supply the water demand, analogous to a "carbon footprint" (32). Total water footprints based on water withdrawals are captured in Fig. 3*A*, where WSI indirectly represents the fraction of a subregion's land area necessary to generate the streamflow to sustain those withdrawals. Here we estimate net agricultural water footprints of the 332 largest US MSAs [>100,000 in population as of 2000 (33)]. Virtual water in food includes water transpired during production [via actual evapotranspiration (AET), i.e., "green water" (14)], is higher in arid regions with higher prevailing rates of evapotranspiration, and is ≈80% of all consumptive water use worldwide (14). Net virtual water represents the difference between virtual water import and export, or alternatively, the difference between the virtual water in locally grown food and the virtual water locally consumed. We define a virtual water footprint (VWF) of a city as the land area necessary to capture the streamflow required to satisfy the net virtual water transfer (i.e., to grow the additional crops needed to feed the population of that city that are not grown locally). Thus, our virtual water footprints differ from WSI in two ways: (*i*) they quantify the total land area equivalents of streamflow needed to feed cities via local agriculture, and (*ii*) they allow us to quantify net virtual trade in terms of import of virtual water to cities (positive VWF) and export of virtual water from watersheds with extensive crop area (negative VWF). Cities in the Desert Southwest United States had disproportionately high net water import (large positive VWF) (Fig. 4*A*). Urban areas with the top five total positive VWF (indicating net imports of virtual water) were Los Angeles, Las Vegas, Phoenix, New York, and Riverside, in that order. The VWF of Los Angeles is larger than the combined VWF of the eight largest VWFs east of the 100th meridian, including New York, Chicago, Dallas, Detroit, Philadelphia, Houston, Boston, and Washington, DC. Combined VWF for these eight metro areas is 206,585.5 km^2, compared with 214,922 km^2 for the Los Angeles metropolitan area. Watersheds exporting the most virtual water in the form of food products typically hosted smaller cities, many in the corn belt (Fig. 4*B*); subregions with the highest net virtual water export were those hosting Wichita (KS), Sioux Falls (SD), Omaha (NE), Havasu City (AZ), and Colorado Springs (CO), in that order. The virtual water demand of these smaller population centers is dwarfed by water used for agriculture in their watersheds, which is exported as food products. Average VWFs were positive west of the 100th meridian (indicating net import) and negative east of the 100th meridian (indicating net export; Fig. 2*H*). Western cities with net positive VWF had 7-fold larger footprints than cities with net positive VWF east of the 100th meridian (Fig. 2*H*). Western watersheds also export 1.7-fold more virtual water than watersheds dominated by cropland east of the 100th meridian (Fig. 2*H*), although this latter difference is not significant (Table S1). In summary, western cities have much larger virtual water footprints, largely owing to the more arid climate, and western crop lands export at least an equal magnitude of virtual water as cities and croplands east of the 100th meridian. Some but not all of the virtual water exported from productive farmland in the western United States (e.g., Central and Imperial valleys of California) offsets large footprints of cities in the desert Southwest, because these farmlands produce table vegetables, tree fruit, and nuts for much of the United States.

Human appropriation of streamflow in the US Southwest. Six major watersheds in the US Southwest are connected by aqueducts and water transfers (Fig. 4*B*). Water from the upper Colorado basin is diverted across the continental divide to the South Platte, Arkansas, and Rio Grande rivers for municipal use by front-range cities as well as agriculture. Snowmelt from the upper Colorado basin is collected lower in the basin and diverted to Las Vegas, central and southern Arizona, and southern California. Snowmelt from the Sierra Nevada is diverted to San Francisco and Reno and to cropland in the southern Central Valley of California via the Central Valley Project (CVP). Finally, snowmelt from the northern Sierra Nevada and water from Trinity River in California's Northern Coast Range is diverted south to the Central Valley (via the CVP), some portion of which reaches southern California via the State Water Project of California. The resulting human-engineered watershed connects streamflow generated in the mountains of Colorado and California to cities in at least six states, representing a combined urban population of more than 50 million, and to one third of all western croplands.

Here we quantify the human appropriation of streamflow in this superregion (Fig. 4*B*). The simplest index of human appropriation is WSI, or withdrawals normalized to MAF across the superregion (*SI Appendix*). Humans currently appropriate the equivalent of 76% of MAF in this superregion (WSI 0.76; Fig. 4*B*). This number is equivalent to >90% of streamflow when we use the virtual water demand for agriculture instead of the actual withdrawals associated with current agricultural practices to calculate WSI (Fig. 4*B*). This "virtual WSI" accounts for all water needed to grow crops to sustain the entire population in the superregion, assuming food is grown within and no food is transported out of the super region (i.e., "regional food production"). Higher virtual WSI suggests that much higher appropriation of streamflow would be

[§]Here we focus on hydrologic regions 13–18, quantifying prevalence of nonnative fishes in 8-digit hydrologic unit code basins or accounting units. We chose a finer resolution for this analysis to illustrate the comprehensive nature of fish invasion in western watersheds. At this finer level of resolution, we can record not only whether a particular nonnative fish is present in a 4-digit subregion but also how widespread it is within that subregion.

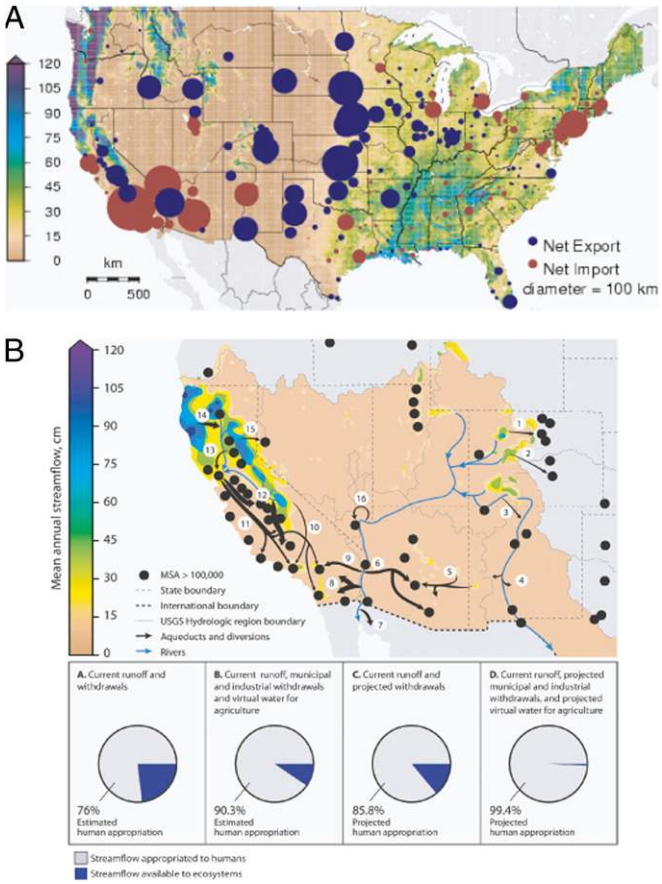

Fig. 4. Water footprints for agriculture and human appropriation of streamflow by urban areas in the US Desert Southwest. (*A*) Net virtual water footprints of metropolitan statistical areas >100,000 in size. Footprints represent the land area equivalent of streamflow generation required to grow the food to feed the MSA population (following ref. 45); positive numbers (blue) indicate net export (i.e., the MSA's hydrologic subregion produces more food than is required by the MSA population), and negative numbers (red) indicate net import (the MSA requires more food than is produced within the local hydrologic subregion) for each MSA. See *SI Appendix* for more details. (*B*) Appropriation of streamflow by large urban areas (Census 2000 MSAs >100,000 in size) under a population doubling scenario of these cities. Map shows the paucity of streamflow across five southwestern USGS hydrologic regions (Regions 13–16 and 18) and the natural and engineered causeways for this streamflow. Pie charts show proportion of streamflow appropriated by large urban areas in the same five-hydrologic-region area under four scenarios. Scenario A is the current water scarcity index (WSI = W/MAF) for the entire five-region area using USGS water use data from 2000 (W). Scenario B estimates the capacity for streamflow to support municipal and industrial withdrawals in Scenario A in addition to the virtual water needed for regional production of all food. The difference in human appropriation between Scenarios A and B highlights the degree to which the Desert Southwest imports streamflow (contained in food) from more distant hydrologic regions. Scenarios C and D project human appropriation of streamflow under a regional doubling scenario of all MSAs >100,000 in size in 2000, assuming only changes in W associated with population increase (*SI Appendix*). In Scenario C, projections are based on water use data (in Scenario A), whereas in Scenario D, projections are based on municipal and industrial withdrawals and estimated virtual water for agriculture. All scenarios rely on current VIC streamflow estimates (MAF, based on average annual climate forcings from 1950 to 1995). Arrow width is proportional to the magnitude of water diversion associated with numbered major water projects in the Southwest: (1) Duchesne River Diversion, (2) Blue, Fraser, and Williams Fork River diversions, (3) Frying Pan and Eagle River diversions, (4) San Juan River diversion, (5) Middle Rio Grande River diversions, (6) Salt River Project, (7) Central Arizona-Phoenix Project, (8) Colorado River flow exiting United States to Mexico (1.85 $km^3 \cdot y^{-1}$) as mandated by The Mexican Water Treaty of 1944, (9) All American Canal, (10) Colorado River Aqueduct, (11) Boulder Canyon Project, Lake Mead, (12) Los Angeles Aqueduct, (13) State Water Project, California Aqueduct, (14) Central Valley Project, (15) Tuolumne River diversion, (16) Truckee River diversions, (17) Central Valley Project: Trinity River diversion.

required for the superregion to persist on locally grown food alone and that there are likely important, but not as of yet quantified, ecological tradeoffs between water footprints associated with regionally produced agriculture and carbon footprints associated with food imports from agricultural lands outside the superregion.

Finally, population in the Cadillac Desert superregion is projected to increase significantly over the next 25–40 y (all projections available from the US Census Bureau; ref. 34). For example, the population of the state of California is projected to grow by 50% by 2050, the population of southern Nevada is projected to grow by as much as 57% by 2030, and the Phoenix metropolitan area (here defined as Maricopa County) and population centers on the Front Range of the Rocky Mountains of Colorado are projected to double by 2050 and 2040, respectively. This suggests that population doubling is possible in many population centers in the superregion within a century. Hence, we estimated WSI and virtual WSI as above, but assuming twice the population in the superregion. Using a conservative (more recent) trend for the relationship between population and water use, we estimate that humans will withdraw ≈86% of current MAF under a population doubling (WSI 0.86). Withdrawals could be as high as 99.4% of current MAF according to the extrapolated virtual water demand required for regional food production (virtual WSI 0.99; Fig. 4*B*).

Discussion

John Wesley Powell provided the earliest sketch of sustainable development in the western United States. Powell's conclusion in 1876 was that water scarcity would place limits on the growth of a new civilization in the region (3). Marc Reisner pursued this conclusion in *Cadillac Desert* a century after Powell's explorations (5). Reisner's diagnosis was that the water demands of agriculture and growing western cities were at odds and precariously dependent on static conditions—optimistic estimates of streamflow, unchanging reservoir storage capacity, and soils buffered against high salt loads. In this article we use data and methods unavailable in Reisner's time to reevaluate this diagnosis. We find that the characteristics and impacts of dams and reservoirs differ considerably between the eastern and western United States, suggesting that the Cadillac Desert envisioned by Marc Reisner has a strong scientific basis. Specifically, the US west of the 100th meridian is characterized by (*i*) low mean annual streamflow; (*ii*) large reservoirs spaced more distantly within river networks, but storing a more than 4-fold higher proportion of mean annual streamflow than in the East; (*iii*) 3-fold higher surface water withdrawals as a proportion of streamflow; (*iv*) net virtual water footprints at least seven times the area of those of eastern cities; (*v*) large reservoirs with estimated minimum lifespans exceeding 1.5–2 centuries that have nevertheless already experienced losses in firm yield greater in volume than the annual conveyance of critical water delivery

systems (e.g., Los Angeles Aqueduct); (*vi*) >60-fold greater reductions in agricultural revenue due to inefficient irrigation practices and soil salinity; and (*vii*) faunas with nearly six times the ratio of nonnative to native fishes than those in the East. Our storyline, although hopefully more measured, is in line with the one Reisner crafted in 1986.

Interaction Between Reclamation and Climate Change. Our synthesis of water resources data ignores important interactions with climate change. Increased temperatures, higher water demand by crops, greater rainfall variability, reduced snowpack and streamflow, earlier snowmelt and peak streamflow timing, and a doubling of major urban populations are very likely scenarios in the next 100 y. Less certain but likely scenarios include reduced average annual precipitation in the southwest United States and climate/population-induced water withdrawal increases. Our analysis provides some insight about interactions between water storage systems, climate change, and population growth scenarios.

First, continued sediment accumulation will result in lower active storage and further reductions in yield of water from reservoirs. Reductions in firm yield due to sediment will be exacerbated by declines in streamflow, increases in variability, and changes in the timing of peak streamflow associated with climate change. Second, agricultural revenue losses due to salinization are likely to rise. Increasing temperatures would increase crop water demand and crop transpiration, leading to greater soil concentration of salts. Seasonal shifts and reductions in western water supply will require greater reliance on saline/brackish or nonrenewable fresh groundwater as a source for irrigation water. This double squeeze, from both supply and demand sides, is expected to increase soil salinization in much of the West. Third, invasion of rivers by nonnative fishes is ongoing. Native species in heavily invaded ecosystems will become increasingly threatened by nonnative species and flow regimes further altered by climate change.

In closing, we note that the capacity for water to support cities, industry, agriculture, and ecosystems in the US West is near its limit under current management practices. For an urban population double the Census 2000 size, we estimate that water withdrawals necessary to meet municipal, industrial, and agricultural demand will exceed 86% of the current streamflow across parts of seven hydrologic regions in the southwest United States (Fig. 4*B* and *SI Appendix*). Our estimate of human appropriation is >99% of the streamflow generated by this region if we include the water needed to produce all food to feed a doubled population in the region (Fig. 4*B*). These estimates are conservative for two reasons. First, our population doubling scenario does not include supply reductions due to climate change. Second, we assume conservative increases in water withdrawals as the urban population grows. Even these most-conservative estimates suggest that renewable freshwater resources will not comfortably support a population beyond two times the current levels in the western United States while still providing adequate flows to maintain vital ecosystems.

To reclaim freshwater sustainability in the Cadillac Desert, we suggest an initially modest target of a 16% reduction in the fraction of streamflow withdrawn, or WSI = 0.6 before the realization of a projected population doubling across the entire geographic region (Fig. 4*B*). This improved regional WSI represents a compromise between reductions that would alleviate water stress altogether (WSI 0.4) and those that would significantly diminish already insufficient freshwater resources in river and delta ecosystems (WSI >0.8). Meeting this target will require a regional water conservation policy coordinated across seven US states addressing at a minimum: (*i*) continued improvements in urban water use efficiency, (*ii*) implementation of desalinization by coastal cities, (*iii*) continued improvements in land-use practices that minimize erosion and sediment infilling of the region's reservoirs, (*iv*) technological advances increasing water application efficiency during irrigation, (*v*) modified crop portfolios that include only salt tolerant and cash crops, (*vi*) effective reallocation of salvaged surface water to ecosystems as farmlands are retired and cities shift to desalinization, and (*vii*) endorsement of market-based rather than government-subsidized water pricing for all uses except those that fulfill the most basic daily human needs. Further, Reisner's book *Cadillac Desert* and our analyses do not consider the impact of water use on groundwater reserves. A regional policy of freshwater sustainability should bridge this gap and (*viii*) implement aquifer storage and recovery and artificial recharge schemes for water storage and management, and (*ix*) endorse only judicious use of groundwater with minimal impact on surface flows in pursuit of our suggested target (WSI 0.6). This regional policy of freshwater sustainability will impose a cost, and this cost—as Reisner noted—will most likely include more expensive water at the tap and on the farm.

Materials and Methods

Macroscale Hydrology. We used a macroscale hydrologic model—the Variable Infiltration Capacity (VIC) model (35, 36)—to quantify patterns in mean annual streamflow volume (km^3) across the coterminous United States at a resolution of 1/8 degree using observed meteorological forcings from 1950 to 1999 (37). We used the VIC model to estimate streamflow (as opposed to available data) because the VIC model provides estimates of virgin flow, whereas empirically measured streamflow includes the effects of withdrawals and river regulation by dams. In contrast to previous continental-scale applications of the VIC model (37–39), the current version was implemented with seasonally frozen soils, improving energy and water balance estimates during the winter season (40, 41). The VIC model was calibrated to monthly naturalized and observed streamflow for 12 watersheds within six major representative hydrologic regions across the coterminous United States for a 10-y period and then evaluated for the remaining (independent) observational period of 10–40 y, between 1950 and 1999. Model bias was low and positive on average (9.2% ± 5.9% of naturalized or observed streamflow) with reasonable variation across basins (Table S3).

Patterns of Infrastructure. Using data from the National Inventory of Dams we summed the total number and storage capacity of reservoirs in each USGS subregion. We then estimated the average number of dams per 100 km of river length [according to USGS's HYDROGL020 layer (US National Atlas Water Feature Areas)] (42) or dam density. We also quantified the total storage capacity relative to mean annual streamflow (*relative* storage capacity) for each subregion using streamflow estimates from the VIC model (Fig. 1). We then made East vs. West comparisons in this section and all others to follow at the watershed, or USGS four-digit hydrologic code (HUC 4) subregion resolution. For all East vs. West comparisons, we used geographic centroids of HUC 4 subregions to determine their location relative to the 100th meridian.

Sediment Infilling. We quantified infilling rates, reservoir storage capacity losses, and lifespans using the RESIS-II database (43). This database includes repeat bathymetric surveys for >1,200 reservoirs in the United States. We estimated single structure storage capacity losses from closure to present (2010). Total capacity losses for hydrologic subregions were then estimated by multiplying the subregion's total reservoir capacity [from the National Inventory of Dams (NID)] by the minimum observed proportion of capacity lost (from RESIS-II). We expressed this capacity loss as a proportion of the subregion's mean annual streamflow (i.e., *relative* capacity loss).

Firm Yield Analysis. For 24 reservoirs in the RESIS-II database ranging in size from 0.04 to 35.5 km^3, we estimated the change in firm yield via sequent peak analysis based on our estimates of current active storage and observed monthly streamflow data from nearby USGS stations.

Agricultural Revenue Losses to Salinity. We estimated revenue losses as a result of diminished crop yields in saline soils for all 204 hydrologic subregions in the coterminous United States. We identified salt-affected soils using the nationwide State Soil Geographic Database (STATSGO). We then estimated revenue losses according to nationwide crop type and soil salinity maps and data on crop salt tolerances, crop yields, and prices.

Fish Invasion. We cataloged patterns of invasion by nonnative fishes using the USGS Nonindigenous Aquatic Species (NAS) database (44) and NatureServe's Distribution of Native Fishes by Watershed database (45). For nonnative fishes in the NAS dataset, we used only established, locally established, and stocked nonnative species in the NAS dataset to avoid spurious single sightings of nonindigenous species that might inflate our estimates of invasion. We recompiled presence/absence data at the resolution of hydrologic subregions in the lower 48 states and estimated α diversity for native, nonnative, and all (native and nonnative) fishes in each subregion (Fig. S4).

Water Footprints. To estimate a water footprint for each city, we used the annual per capita water requirements based on a published average US diet (46). We also calculated per capita crop water use for each subregion using estimates of AET from cropped areas under natural rainfall together with known quantities of irrigation water withdrawals. Per capita values were multiplied by the MSA population size from the 2000 census (US Census Bureau). The difference in virtual water demand and supply was normalized by streamflow depth from the VIC model to estimate the land area required to capture the net virtual water demand.

Extrapolation of Human Appropriation of Streamflow Under Population Doubling. To extrapolate water use and human appropriation of streamflow under a population doubling scenario, we developed a regression relationship between total US population size and total annual water withdrawals. The slope of this relationship at the time of publication of Cadillac Desert was $\approx$2, indicating a doubling in water extraction with population growth. Estimates of water withdrawals over the last 25 y (1980–2005) indicate that withdrawals have increased much less dramatically with population (slope = 0.23 per unit population). We extrapolate WSI and virtual WSI under a population doubling scenario for the superregion assuming a constant relationship between water use and population (slope = 0.23) over time frames consistent with population doubling (40–90 y). We recognize the perils of linear extrapolation of current water rates and thus rely on the more conservative, flatter relationship between population and water withdrawals to estimate future WSI.

ACKNOWLEDGMENTS. We thank J. Baron, N. Baron, G. Basile, R. Glennon, J. Holway, T. Lant, C. Magirl, C. Perrings, S. Postel, R. Reeves, M. Scott, J. Reichman, and M. Wright for ideas, encouragement, data processing, and constructive comments on previous versions of the manuscript. J.L.S. thanks S. Bacon, J. Elser, J. Fink, and P. Gober for funding via Arizona State University (ASU)'s College of Liberal Arts and Sciences, the School of Life Science Research and Training Initiatives Office, the Global Institute of Sustainability, and the Decision Center for a Desert City, respectively. This project was supported by National Science Foundation Grant EAR-0756817 (to J.L.S.) and ASU's Office of the Vice President for Research and Economic Affairs. This work was conducted as a part of the "Sustainability of Freshwater Resources in the United States" Working Group supported by the National Center for Ecological Analysis and Synthesis, a center funded by National Science Foundation Grant EF-0553768, the University of California, Santa Barbara, and the State of California.

1. Powell JW (1890) The irrigable lands of the arid region. *Cent Mag* 39:766–776.
2. de Buys W (2001) *Seeing Things Whole: The Essential John Wesley Powell* (Island Press, Washington, DC).
3. Powell JW (1876) *A Report on the Arid Regions of the United States, with a More Detailed Account of the Lands of Utah* (US Government Printing Office, Washington, DC).
4. Graf WL (1999) Dam nation: A geographic census of American dams and their large-scale hydrologic impacts. *Water Resour Res* 35:1305–1311.
5. Reisner M (1986) *Cadillac Desert: The American West and its Disappearing Water* (Penguin Books, New York).
6. US Census Bureau (2008) *Population of the 100 largest cities and other urban places in the United States: 1790 to 1999*. Available at http://www.census.gov/population/www/documentation/twps0027/twps0027.html. Accessed November 30, 2010.
7. City Mayors (2010) *The fastest growing US cities: Cities ranked 1 to 100*. Available at http://www.citymayors.com/gratis/uscities_growth.html. Accessed November 30, 2010.
8. US Department of Agriculture (2010) *National agricultural statistics service*. Available at http://www.nass.usda.gov/QuickStats/indexbysubject.jsp?Pass_-group=Economics. Accessed November 30, 2010.
9. Glennon RJ (2002) *Water Follies: Groundwater Pumping and the Fate of America's Fresh Water* (Island Press, Washington, DC).
10. Glennon RJ (2009) *Unquenchable: America's Water Crisis and What To Do About It* (Island Press, Washington, DC).
11. Pearce F (2007) *When the Rivers Run Dry—The Defining Crisis of the 21st Century* (Beacon Press, Boston).
12. Worster D (1986) *Rivers of Empire: Water, Aridity, and the Growth of the American West* (Pantheon Books, New York).
13. Seaber PR, Kapinos FP, Knapp GL (1987) *Hydrologic Unit Maps: U.S. Geological Survey Water-Supply Paper 2294* (USGS, Reston, VA).
14. Oki T, Kanae S (2006) Global hydrological cycles and world water resources. *Science* 313:1068–1072.
15. Gliek PH (1990) Vulnerabilities of water systems. In *Climate Change and U.S. Water Resources*, ed Waggoner P (J. Wiley and Sons, New York), pp 223–240.
16. U.S. Geological Survey (2010) *Estimated use of water in the United States county-level data for 2005*. Available at http://water.usgs.gov/watuse/data/2005/. Accessed November 30, 2010.
17. Ghassemi F, Jakeman AJ, Nix HA (1995) *Salinisation of Land and Water Resources: Human Causes, Extent, Management and Case Studies* (Univ New South Wales Press, Sydney).
18. Vörösmarty CJ, et al. (2010) Global threats to human water security and river biodiversity. *Nature* 467:555–561.
19. Anonymous (2009) *North Pacific Salmon Fisheries Economic Measurement Estimates* (Wild Salmon Center, Portland, OR).
20. Carpenter SR, Kitchell JF (1988) Consumer control of lake productivity. *Bioscience* 38:764–769.
21. Schindler DE, Carpenter SR, Cole JJ, Kitchell JF, Pace ML (1997) Influence of food web structure on carbon exchange between lakes and the atmosphere. *Science* 277:248–251.
22. Guegan JF, Lek S, Oberdorff T (1998) Energy availability and habitat heterogeneity predict global riverine fish diversity. *Nature* 391:382–384.
23. Muneepeerakul R, et al. (2008) Neutral metacommunity models predict fish diversity patterns in Mississippi-Missouri basin. *Nature* 453:220–222.
24. Poff NL, Olden JD, Merritt DM, Pepin DM (2007) Homogenization of regional river dynamics by dams and global biodiversity implications. *Proc Natl Acad Sci USA* 104:5732–5737.
25. Sabo JL, Finlay JC, Kennedy T, Post DM (2010) The role of discharge variation in scaling of drainage area and food chain length in rivers. *Science* 330: 965–967.
26. Johnson PTJ, Olden JD, Vander Zanden MJ (2008) Dam invaders: Impoundments facilitate biological invasions into freshwaters. *Front Ecol Environ* 6:359–365.
27. Stohlgren TJ, et al. (2006) Species richness and patterns of invasion in plants, birds, and fishes in the United States. *Biol Invasions* 8:427–447.
28. Bestgen KR, Bundy JM (1998) Environmental factors affect daily increment deposition and otolith growth in young Colorado squawfish. *Trans Am Fish Soc* 127:105–117.
29. Seegrist DW, Gard R (1972) Effects of floods on trout in Sagehen Creek, California. *Trans Am Fish Soc* 101: 478–482.
30. Halpern BS, et al. (2008) A global map of human impact on marine ecosystems. *Science* 319:948–952.
31. Hoekstra AY, Champaign AK (2008) *Globalization of Water: Sharing the Planet's Freshwater Resources* (Blackwell Publishing, Oxford).
32. Wackernagel M, Rees W (1996) *Our Ecological Footprint: Reducing Human Impact on Earth* (New Society Publishers, Philadelphia).
33. US Census Bureau, Population Division (2010) *Metropolitan and micropolitan statistical areas*. Available at http://www.census.gov/population/www/metroareas/metrodef.html. Accessed November 30, 2010.
34. US Census Bureau, Population Division (2010) *US population projections*. Available at http://www.census.gov/population/www/projections/st-prod-proj-list.html. Accessed November 30, 2010.
35. Liang X, Lettenmaier DP, Wood EF (1996) One-dimensional statistical dynamic representation of subgrid spatial variability of precipitation in the two-layer variable infiltration capacity model. *J Geophys Res* 101(D16):21403–21422.
36. Liang X, Lettennmaier DP, Wood EF, Burges SJ (1994) A simple hydrologically based model of land surface water and energy fluxes for general circulation models. *J Geophys Res* 99(D7):14415–14428.
37. Maurer EP, Wood AW, Adam JC, Lettenmaier DP, Nijssen B (2002) A long-term hydrologically based dataset of land surface fluxes and states for the conterminous United States. *J Clim* 15:3237–3251.
38. Mitchell KE, et al. (2004) The multi-institution North American Land Data Assimilation System (NLDAS): Utilizing multiple GCIP products and partners in a continental distributed hydrological modeling system. *J Geophys Res* 109:1–32.
39. Nijssen B, O'Donnell GM, Lettenmaier DP, Lohmann D, Wood EF (2001) Predicting the discharge of global rivers. *J Clim* 14:3307–3323.
40. Cherkauer KA, Bowling LC, Lettenmaier DP (2003) Variable infiltration capacity (VIC) cold land process model updates. *Global Planet Change* 38:151–159.
41. Cherkauer KA, Lettenmaier DP (1999) Hydrologic effects of frozen soils in the upper Mississippi River basin. *J Geophys Res* 104:19599–19610.
42. United States National Atlas (2010) *Streams and waterbodies of the United States*. Available at http://nationalatlas.gov/mld/hydrogm.html. Accessed November 30, 2010.
43. Water Information Coordination Program (2010) *The reservoir sedimentation database (RESSED)*. Available at http://ida.water.usgs.gov/ressed/background/index.cfm. Accessed November 30, 2010.
44. United States Geological Survey (2010) *NAS-nonindigenous aquatic species*. Available at http://nas.er.usgs.gov/. Accessed November 30, 2010.
45. NatureServe (2010) *Distribution of native US Fishes by Watershed*. Available at http://www.natureserve.org/getData/dataSets/watershedHucs/index.jsp. Accessed November 30, 2010.
46. Renault D, Wallender WW (2000) Nutritional water productivity and diets: From "crop oer drop" towards "Nutrition per drop". *Agric Water Manage* 45: 275–296.

Supplementary Information

Supplementary Figures & Tables referenced in the text

Figure S1: A - Total reservoir capacity in units of acre feet for each hydrologic subregion (log base 10 transformed), and **B -**Frequency distributions of closure dates and storage capacities of reservoirs from RESIS II estimated to have completely filled with sediment east and west of 100th Meridian

A

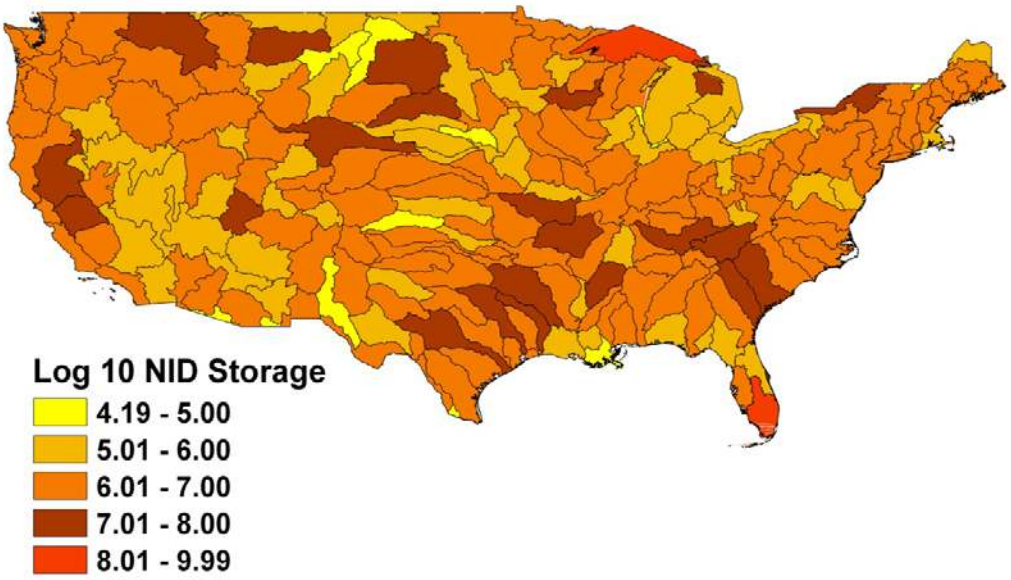

B

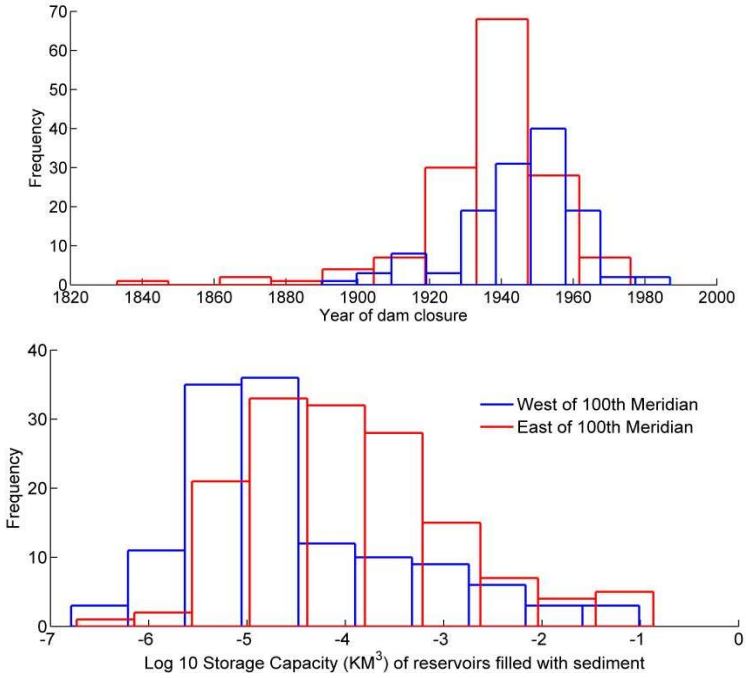

Figure S2: A - Upper and lower confidence bounds of lifespans (text) and number of reservoirs estimated to have completely filled with sediment (color) in each hydrologic region, based on data from RESIS II, and **B** - Relationships between active storage and firm yield estimated via sequent peak analysis for 24 US reservoirs.

A

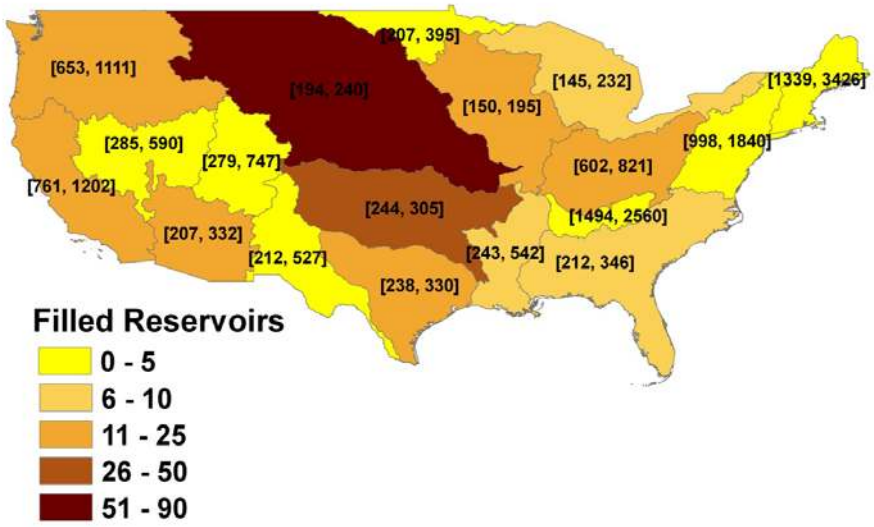

B

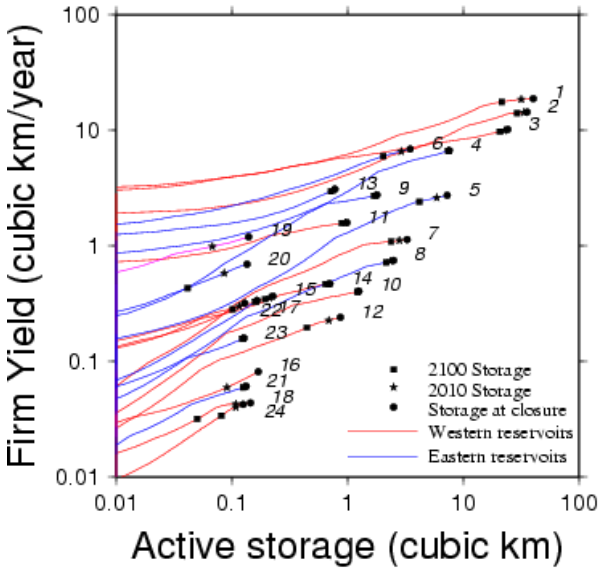

1) Lake Mead, NV
2) Lake Powell, UT
3) Ft Peck Lake, MT
4) Lake Cumberland, KY
5) Lake Texoma, OK
6) John Kerr Reservoir, VA
7) Elephant Butte Reservoir, MT
8) Lake Whitney, TX
9) Fontana Lake, NC
10) Pine Flat Lake, CA
11) Glendo Reservoir, WY
12) John Martin Resrvoir, CA
13) Bluestone Lake, WV
14) Lake Isabella, CA
15) Bartlett Lake, AZ
16) Angostura Reservoir, SD
17) Tionesta Reservoir, PA
18) Jemez Canyon Reservoir, NM
19) Jackson Lake, GA
20) Ocoee Lake, TN
21) Fort Supply Lake, OK
22) Gibson Lake, MT
23) Deer Creek Reservoir, OH
24) LakePiru, CA

Figure S3: Salt affected soils in the US in red (from STASGO) and croplands in green. Hydrologic subregions with salt accumulation/depletion are indicated with rose/yellow background shades. Subregions shaded black indicate inadequate data to estimate salt budgets.

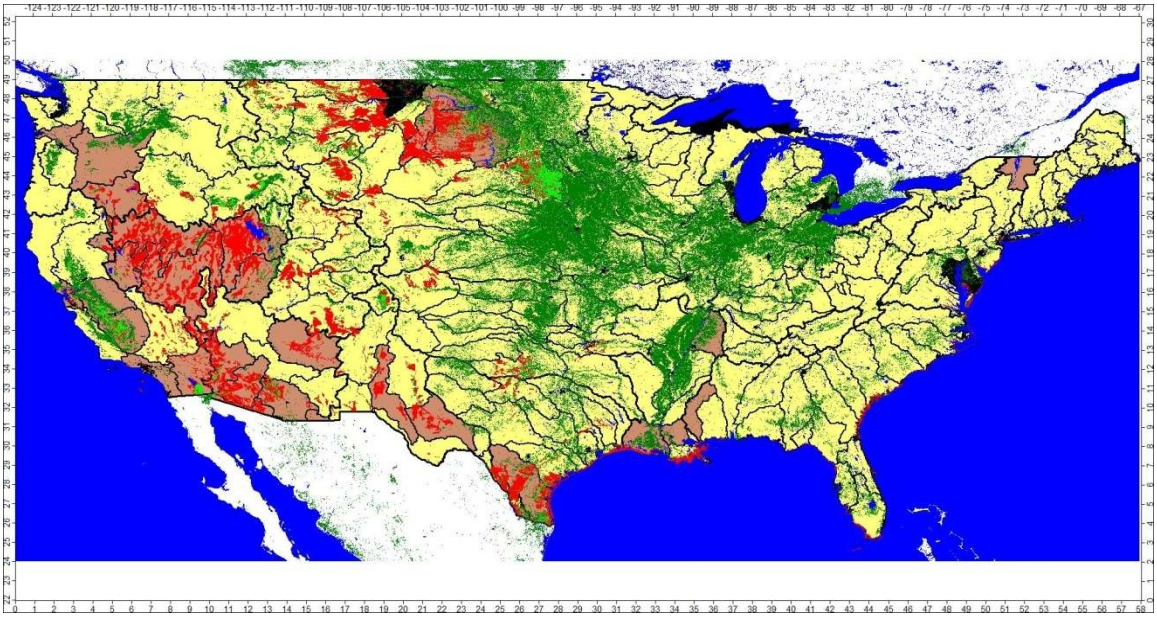

Figure S4: Number of native fishes in hydrologic subregions of the coterminous US

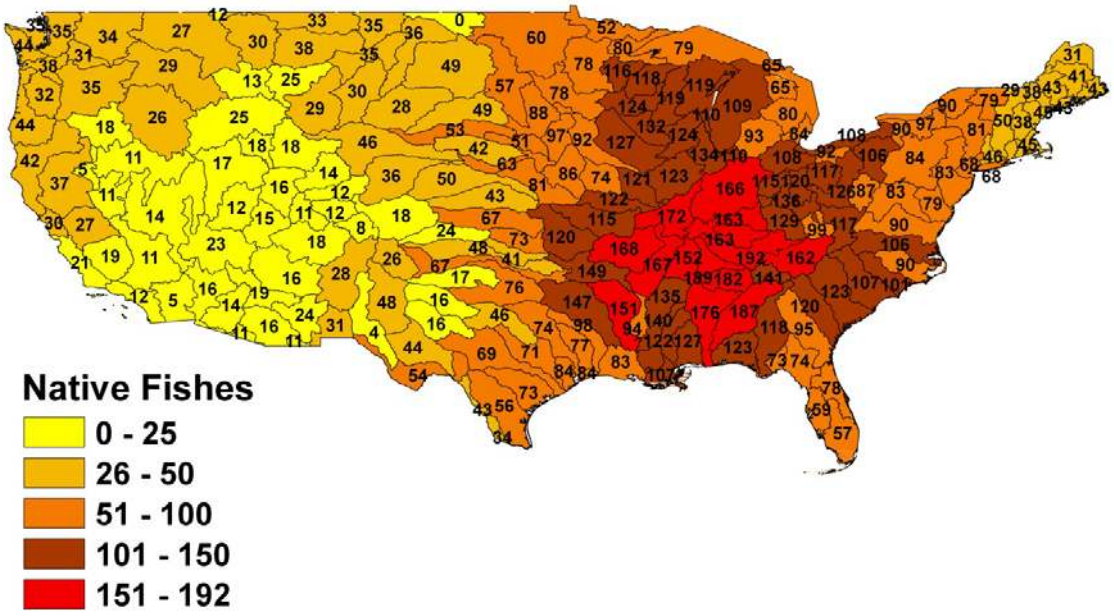

Table S1: Data analysis: Student's *t*-tests comparing attributes and impacts east and west of 100th Meridian. E and W denote values for subregions East and West of the 100th Meridian. SD is standard deviation and *t* and P are the Student's *t*-statistic and significance level for the E *vs*. W comparison.

Attribute	Mean E	Mean W	SD E	SD W	df†	t	P
Acres cropland	2004241	1148403	2556084	1336440	202.00	-2.72	0.01
Current estimated reservoir storage loss expressed as a fraction of total streamflow	0.27	1.10	0.10	0.51	79.60	13.98	0.00
USD lost (average)	4068195	4572759	18047149	8454431	202.00	0.23	0.82
USD lost (average) standardized by acres of cropland	2.26	9.27	10.48	27.62	89.44	2.14	0.03
Ratio of Non-Native to Native Fishes	0.75	2.25	2.55	4.51	105.93	2.66	0.01
Number of non-native fish species	20.12	24.69	11.99	11.97	202.00	2.64	0.01
Storage	3.89	5.77	5.52	7.71	202.00	2.02	0.04
Storage:Streamflow	1.24	5.00	4.28	10.27	92.22	3.05	0.00
Dams per 100 km	9.91	6.08	8.96	6.47	202.00	-3.27	0.00
Firm yield reduction (large reservoirs)	-0.1035	-0.1168	0.1414	0.1260	7.8957	-0.1571	0.8791
Firm yield reduction (small reservoirs)	-0.0626	-0.0096	0.0859	0.0079	5.0642	1.5065	0.1578

†Degrees of freedom are identical for all tests where we observed homogeneity of variances ($SD_W/SD_E < 2.5$), $N_e = 127$ subregions (watersheds) with centroids E of the 100th Meridian, and $N_w = 77$ subregions with centroids W of the 100th Meridian. Hence, $df = N_e + N_e - 2 = 202$. Where variances were heterogeneous, we used the Brown-Forsythe method to correct the error degrees of freedom when estimating the probability of the observed t-statistic. € Log-10 transformation used to homogenize variance

Table S2. Trophic position and native habitat of 25 most prevalent non-native fish species in 8-digit hydrologic accounting units within hydrologic regions 13-18.

Genus species	Common name	Prevalence (US)	Prevalence (Regions 13-18)	Eastern slow water or lentic species	Piscivorous	Top predator
Micropterus salmoides	Largemouth bass	392	235	Yes	Yes	Yes
Lepomis macrochirus	Bluegill	345	194	Yes	Yes	No
Pomoxis nigromaculatus	Black crappie	373	173	Yes	Yes	No
Cyprinus carpio	Common carp	820	171	No	No	No
Pomoxis annularis	White crappie	310	165	Yes	Yes	No
Micropterus dolomieu	Smallmouth bass	340	163	Yes	Yes	Yes
Ictalurus punctatus	Channel catfish	287	159	Yes	Yes	Yes
Oncorhynchus mykiss	Rainbow trout	414	145	No	Yes	Yes
Salmo trutta	Brown trout	377	139	No	Yes	Yes

Perca flavescens	Common perch	221	133	No	No	No
Ameiurus nebulosus	Brown bullhead	156	128	Yes	Yes	No
Salvelinus fontinalis	Brook trout	182	101	No	Yes	No
Lepomis cyanellus	Green sunfish	176	88	Yes	Yes	No
Sander vitreus	Walleye	287	86	Yes	Yes	Yes
Gambusia affinis	Gambusia	115	82	No	No	No
Lepomis gibbosus	Pumpkinseed sunfish	126	82	Yes	Yes	No
Ameiurus melas	Black bullhead	94	71	Yes	Yes	No
Morone saxatilis	Striped bass	176	66	No	Yes	Yes
Pimephales promelas	Fathead minnow	159	63	Yes	No	No
Esox lucius	Northern pike	113	50	Yes	Yes	Yes
Ctenopharyngodon idella	Grass carp	304	48	No	No	No
Ameiurus natalis	Yellow bullhead	63	47	Yes	Yes	No
Oncorhynchus nerka	Kokanee salmon	65	44	No	No	No
Salvelinus namaycush	Lake trout	79	44	Yes	Yes	Yes

Table S3: Comparison of naturalized (shown in italics) or observed streamflow with the VIC model simulated streamflow at selected gauging sites. Calibration statistics are represented in bold.

Site	River Basin Name	Fraction of basin area	% Bias [NS*] 1950-59	% Bias [NS*] 1960-69	% Bias [NS*] 1970-79	% Bias [NS*] 1980-89	% Bias [NS*] 1990-99
IMPER	*Colorado*	*0.74*	***-9.4***	*-22.8*	*-12.4*	*-0.31*	*4.7*
			[0.58]	*[0.64]*	*[0.52]*	*[0.43]*	*[0.47]*
CISCO	*Colorado*	*0.09*	***-20.9***	*-32.0*	*-22.0*	*-20.4*	*-20.7*
			[0.72]	*[0.80]*	*[0.82]*	*[0.77]*	*[0.80]*
GREUT	*Colorado*	*0.18*	***-2.5***	*-24.5*	*-23.0*	*1.6*	*-0.61*
			[0.48]	*[0.76]*	*[0.71]*	*[0.36]*	*[0.46]*
PRIES	*Columbia*	*0.44*	*20.8*	***11.8***	*9.1*	*16.4*	-
			[0.04]	***[0.27]***	*[0.41]*	*[0.00]*	
CHIEF	*Columbia*	*0.35*	*15.1*	***4.8***	*2.5*	*11.2*	-
			[0.27]	***[0.43]***	*[0.56]*	*[0.24]*	
ALTON	Upper Mississippi	1.0	27.9 [0.39]	23.4 [0.57]	9.6 [0.74]	***5.2*** ***[0.68]***	*0.62* *[0.66]*[#]
KEOKR	Upper Mississippi	0.70	32.4 [0.16]	26.7 [0.43]	16.7 [0.63]	***9.9*** ***[0.62]***	*3.6* *[0.60]*[#]
LITLR	Arkansas	0.69	22.6 [0.77]	42.1 [0.21]	-	-	***34.8*** ***[0.70]^***
GARIS	*Missouri*	*0.37*	*-9.6*	***-9.4***	-	-	-

			[-0.63]	***[0.02]***			
FTPCK	*Missouri*	*0.19*	*-3.2*	***2.0***	-	-	-
			[-1.8]	***[-1.9]***			
WABAS	Ohio	0.14	**-6.6**	-10.8	-12.0	-9.6	-2.5
			[0.79]	[0.72]	[0.73]	[0.73]	[0.83]
SCIOT	Ohio	0.03	**20.1**	11.3	5.2	12.2	16.0
			[0.71]	[0.82]	[0.69]	[0.74]	[0.75]

*NS is Nash-Sutcliffe Efficiency [shown in brackets], #1990-1998, ^1987-1995

Sites represent: IMPER - Colorado River above Imperial Dam, AZ; CISCO – Colorado River near Cisco, UT; GREUT – Green River near Green River, UT; PRIES – Columbia River at Priest Rapids Dam, WA; CHIEF: Columbia River at Chief Joseph Dam, WA; ALTON - Mississippi River at Alton, IL; KEOKR - Mississippi River at Keokuk, IA; LITLR - Arkansas River at Little Rock, AR; GARIS - Missouri River at Garrison Dam, ND; FTPCK - Missouri River below Fort Peck Dam, MT; WABAS - Wabash River at Mt. Carmel, IL; and SCIOT - Scioto River at Higby, OH.

Methods:

Table of contents

Description of methods for the following figures from the main body of the paper appear in the following numbered order:

Methods:

1. Macroscale hydrology—Variable Infiltration Capacity (VIC) Model

a. Overview and setup

The Variable Infiltration Capacity model (S1-3) is a physically based land surface model which simulates the full energy and water balance at the earth's surface using three vertical soil layers. The model is implemented using daily precipitation, maximum and minimum air temperature, and wind speed (details described in (S4). A stand-alone routing model (S5, 6) is used to route runoff and baseflow to the basin outlet using the main direction of flow. The VIC model has been widely applied at various spatial scales including river basins, regional, continental and global scales under varied climatic conditions (S4-18).

In the present study, the VIC model version 4.1.1 was implemented at 1/8° by 1/8° latitude by longitude. The finite difference soil thermal solution described by Cherkauer and Lettenmaier (S1) with a constant bottom boundary temperature at the thermal damping depth of 10 m was used. The model was allowed to run for 5 years as a spin up period to reach equilibrium conditions before being implemented from 1950-1999 for the lower 48 states in the US.

b. Model input dataset

The meteorological forcing data from 1950-1999, including daily precipitation, maximum and minimum air temperature and wind speed, were obtained from the Surface Water Modeling Group at the University of Washington from their website at http://www.hydro.washington.edu/Lettenmaier/Data/gridded/, details of which are described in the Land Data Assimilation System (LDAS) project (S4, 14). Soil parameters were gridded at

1/8° by 1/8°scale and were processed from a multilayer soil characteristics data available at 1 km resolution for the conterminous US (CONUS-SOIL), which was originally based on State Soil Geographic (STATSGO) database (S19). Vegetation parameters were obtained from the LDAS project (S4).

c. Calibration and evaluation summary

The VIC model was calibrated for six major river basins (Columbia, Colorado, Missouri, Arkansas, Ohio and Upper Mississippi) at 12 selected streamflow gauging sites based on data availability, 7 with naturalized streamflow and 5 sites with observed streamflow, which were minimally influenced by major dams and reservoirs (Table S3). The model was calibrated for a period of about 10 years, with the period varying for diffwackerent river basins, based on the availability of naturalized or observed streamflow records. The calibrations were performed to improve the agreement of monthly volume and hydrograph shape of observed and simulated streamflow hydrographs. The model was then evaluated for independent time periods that ranged from 10 years (for 2 sites) up to 40 years (for 7 sites) at all 12 sites. We estimated the percent bias and Nash-Sutcliffe (NS) efficiency (S20) for monthly streamflow during the evaluation period and the NS efficiency was acceptable (more than 0.50) for two-thirds of the selected gauging sites. In addition to individual station values, we estimated an overall average percent bias for each river basin over all evaluation periods by accounting for weighted fractional drainage area of all the selected sub-basins located within that river basin. Bias is positive (over-estimating streamflow) but less than 10% on average across all six validation basins (9.2 ± 5.9 % mean annual streamflow depth). Both negative and positive bias was observed for the six validation basins. Specifically, the VIC model over-predicted streamflow in many wet regions, e.g. the Columbia River (13.0%) and the Upper Mississippi (15.8%), whereas underestimates were more frequent in arid regions with hydrographs driven by snowmelt: Colorado (-9.0%) and Missouri (-7.4%). The biggest outlier was the Arkansas basin with overestimation of streamflow by 32%, where poorly documented water withdrawals and diversions may affect the observed flows used for calibration and validation leading to over-prediction by the VIC model (S4). The calibrated parameters for the other basins/regions were chosen from one of the six proximate (selected) river basins with similar hydroclimatological conditions.

d. Methods documentation

Simulation of surface water hydrology for the coterminous US using the VIC model was previously published by Mauer et al. (S4). The primary differences in this application include inclusion of spatially varying soil depth based on the CONUS soil database and use of the soil frost algorithm of Cherkauer and Lettenmaier (S1). In Maurer et al. (2002) total soil depth was determined by basin specific calibration and soil freezing was not represented. The Cherkauer and Lettenmaier algorithm has been used in several publications in cold regions (S21-23) and has been shown to improve model performance in cold regions, relative to the original VIC model (S1). As a result of these two changes, the VIC empirical infiltration and baseflow parameters were also adjusted. In the original Maurer et al. publication, percent bias for twelve gauging sites ranged from -50.9% to 35% during the calibration period. In our revised calibration, percent bias for a different 12 sites ranged from -30.9% to 34.8%, a noticeable improvement.

2. National Inventory of Dams—storage per streamflow and dam density

a. Data sources

National Inventory of Dams: (NID): The National Inventory of Dams dataset maintained by the Army Corps of Engineers (http://crunch.tec.army.mil/nidpublic/webpages/nid.cfm). This dataset includes > 75,000 dams in the US creating water bodies ranging in size from small ponds to large reservoirs (e.g., Lake Mead storage capacity ~40 km^3). NID fields include spatial coordinates, storage capacity and surface area, among other useful entries.

HYDROGL020*:* U.S. National Atlas Water Feature Areas maintained by the U.S. Geological Survey (http://nationalatlas.gov/mld/hydrogm.html).

Hydrologic Unit Code (HUC) – 2 and 4 digits Shapefiles: Hydrologic Unit Codes (HUC) was delineated by the US Geological Survey to divide drainage basins in the US into a national standard hierarchical system based on surface hydrologic features (http://water.usgs.gov/GIS/huc.html). The major divisions of the hydrologic units in the coterminous US include 18 regions (2-digit HUCs, or HUC 2), 204 subregions (4-digit HUCs, or HUC 4) and 2022 accounting units (8-digit HUCs, or HUC 8). The data for 2, 4 and 8-digit HUCs were obtained from US Geological Survey in Environmental Systems Research Institute, Inc. (ESRI) shapefile format.

b. Methods

We identified dams/reservoirs within each HUC 4 hydrologic subregions and summed the storage of all reservoirs for each subregion in the coterminous US. In doing this we ignored levees and water works, focusing on dams that create storage reservoirs on river systems. We then estimated the ratio of total reservoir storage to streamflow within each subregion using estimates of streamflow from the VIC model (Section 1). Finally, we estimated dam density as the number of dams per 100 km of river length in each hydrologic subregion. Using the HYDROGL020 layer, we estimated the length of river (in km) within each subregion. Dam density was estimated as the ratio of dams to river length within each subregion expressed in units of 100 river km as: $Dam\ Density = 100 * (\#\ Dams / River\ Length)$.

3. Estimation of water scarcity index, *WSI*

a. Data sources

Estimated Water Use (2000) —Estimated fresh water use at the county level for 2000 was obtained from (http://water.usgs.gov/watuse/data/2000/index.html) published by the United States Geological Survey (S24). State water agencies self-report total water withdrawals at the county level from both surface and ground water sources in five categories of use for all States: public supply, domestic, irrigation, industrial, and thermoelectric power.

b. Methods

Some pre-processing of the Water Use data was necessary to estimate total surface and groundwater withdrawals for every county in the coterminous US. Several states did not report estimates of domestic self-supplied water withdrawals at the county level, but they did report state totals. The county level withdrawals were estimated based on the proportion of state population in each county for CT, KY, ME, OR, PA, TN, TX, UT and WV. Since this category reflects in-home water use for households that are not on a public supply, this technique is most likely to result in an overestimate of self-supplied withdrawals in urban counties (that have

public supplies) in these states. Livestock, aquaculture, and mining self supplied withdrawals were only compiled for selected States that represented the majority of withdrawals for these categories in 1995. These withdrawals were assumed to be zero for States that did not report in 2000. Aquaculture withdrawals were therefore assumed to be zero in: AK, AZ, CO, CT, DC, IL, IN, IA, KY, ME, MA, MI, MN, MT, NE, NV, NM, NY, ND, OR,PA, RI, SC, SD, TN, TX, VT, VA, WA, WV, and WY. Livestock withdrawals were not reported for: AL, AK, AZ, AR, CO, CT, DC, KY, ME, MA, MS, MT, NV, MH, NM, NY, ND, OR, PA, RI, SC, TN, UT, VT, VA, WA, WV, AND WY. Mining withdrawals were not reported and assumed to be zero in AL, CO, CT, DE, DC, ID, IL, KY, LA, ME, MA, MI, MS, MT, NV, NM, NY, ND, OR, RI, SC, SD, TN, VT, VA, WA, WV, and WI. Any public-supplied withdrawals for these activities are captured in the public supply category for all states.

Total surface and groundwater withdrawals in Mgal/day were normalized by county area and converted to a raster file 1/8° resolution with units of Mgal/day/km^2. The normalized withdrawals multiplied by the land area of a 1/8° cell were then summed over each HUC 4 subregion in the coterminous US (section 2), to find the total subregion water volume. This methodology preserves the volume of total withdrawals, while distributing them spatially. Assuming that total withdrawals are homogeneous throughout a county can lead to some irregularities in western counties that may exceed the size of hydrologic unit boundaries. These errors were neglected, with one exception. Withdrawals from the Lower Colorado River through the All American Canal take place in Imperial County, CA. These withdrawals were attributed to La Paz County, AZ for this analysis, so that the withdrawals would be reflected in the appropriate hydrologic unit.

Estimates of streamflow within each subregion from the VIC model (Section 1) reflect the locally generated water supply. To account for the contribution of upstream water supply in downstream watersheds, upstream and downstream subregions were identified manually based on the dominant river systems. Streamflow from upstream subregions, less total subregion surface water withdrawals, was added to the streamflow in the downstream subregion to generate subregion mean annual flow (MAF). The final figure represents the ratio of total freshwater withdrawals (*W*, both surface and groundwater withdrawals) divided by estimated renewable water supply (MAF), or $WSI = W/MAF$.

c. Caveats

The water use dataset reflects the location of water withdrawals, rather than the destination of extracted water (to the user). Water transfers from rural mountainous regions to urban lowlands, for example will create distortions in the distribution of water withdrawals. Consumptive use values were not estimated in 2000, such that our estimates of *WSI* include consumptive and non-consumptive withdrawals of freshwater. Non-consumptive water withdrawals include several industrial categories including "open-loop" thermo-electric power generation, where water is passed through heat exchangers once for cooling and returned to the source. Thermo-electric power generation accounted for 41% of all freshwater withdrawals in the US in 2005, and 92% of these withdrawals occurred for use in open-loop facilities in which consumptive use is typically < 5% (S25). Freshwater withdrawals for thermo-electric power generation were low in all states west of the 100th Meridian, and highest in Illinois, Texas, Michigan and Tennessee. Thus, while our *WSI* estimates accurately reflect human extraction of freshwater, some fraction of this extracted water may be returned to the stream downstream after use. Nevertheless, *WSI* still reflects stress imposed on ecosystems by the multiple reuse of water within a river system.

4. Basic methods for estimating infilling to 2010 for RESIS II reservoirs

a. Data sources

Reservoir Sedimentation Survey Information System (RESIS II): The database is the most comprehensive database of reservoir sedimentation surveys in the conterminous US (S26). The RESIS II database used in the present study includes data of 6,617 dams, ranging from farm ponds to the largest reservoirs such as Lake Mead. Records are based on surveys conducted for irregular time periods from 1755 to 1993.

b. Methods

Sedimentation and infilling rates were estimated using the RESIS II database in four steps. First infilling for each reservoir was calculated as:

$$I = \frac{S_2 - S_1}{T} \text{ , in } km^3 * yr^{-1} \quad (1)$$

where, I = infilling rate, S_t = sediment volume in year t, T = time (yr) elapsed between surveys (S_1 and S_2). For dams with data for multiple time periods, an average sedimentation infilling rate was estimated using the full length of observations.

Second, the total life span of each dam was extrapolated linearly (assuming homogeneity of infilling rates within subregions) by determining the ratio of total capacity of the reservoir and sedimentation rate per year (1). For example, if sedimentation infilling rate is 2% storage loss per year for a reservoir, then the total life span of the dam is 1/0.02 = 50 years, or:

$$Lifespan = \frac{Max\ Capacity}{I}, units = \left(\frac{(km^3)}{\left(\frac{km^3}{yr}\right)} \right) = yr \quad (2)$$

Third, the remaining life span of a dam was computed as:

$$Lifespan\ remaining = Lifespan - \left(2009 - Y_{closure}\right) \quad (3)$$

where $Y_{closure}$ is the closure date (year) of the dam.

Fourth, since the distribution of the remaining life span of dams was skewed, the data were logarithmically transformed to obtain normal distribution (S27). Thus, 95% confidence intervals ($CI_{transformed}$) for the remaining life span of active dams (excluding completely filled dams) within each 2-digit HUC (Figure S2A) and 4-digit HUC as:

$$CI_{transformed} = \left(\overline{Y} + \frac{S}{2} \right) \pm \left(\sqrt{\left[\left\{ \frac{S}{2} \right\} + \left\{ \frac{S^2}{2(n-1)} \right\} \right]} \right) \quad (4)$$

Where $\overline{Y}$ = ln[remaining life span of active dams], S = standard deviation, and n = number of active dams in the region or subregion. Finally, the CI was estimated using anti-logarithmic natural transformation of the HUC 2 and HUC 4 $CI_{transformed}$.

c. Caveats

Although the RESIS II database has valuable information for reservoir sedimentation, interpretation and extrapolation of the data may be limited for any of the following reasons: 1) some reservoirs do not have precise location coordinates (S28), 2) there is a decline in sedimentation surveys after 1980's, and 3) many larger reservoirs with storage capacities more than 0.123 km^3 were not included in the surveys due to the interest of federal and state agencies in smaller dams and regions with higher soil erosion (S29). We make several assumptions when estimating total infilling rates from dam closure to present based on subsamples of this time series. Specifically, we assume temporal homogeneity in infilling rates or that the sediment surveys conducted prior to 1980's are representative of reservoir sedimentation characteristics currently. Moreover, since the focus of surveys in RESIS-II was on smaller reservoirs in regions with high infilling rates, we may overestimate the severity of infilling.

5. Extrapolation methods for relative storage losses by HUC 2

a. Data sources

Our data sources were the same as in Section 4. The RESIS-II dataset did not include enough large reservoirs to allow us to extrapolate from a single large-structure minimum infilling rate to storage losses within each HUC 4 sub-region. Hence, we extrapolated region-wide (HUC 2) storage losses by applying the minimum observed infilling rate within each hydrologic region to all reservoirs in that HUC 2.

b. Methods

The goal of this section of our work was to estimate the sum of capacity losses for all reservoirs in a hydrologic region (HUC 2) from dam closure to 2010 by extrapolation from point estimates within the same region. To estimate basin wide capacity loss, we used data from the RESIS II Dataset to calculate annual infilling rates ($\propto$ capacity loss rates) and the proportion of the original storage capacity lost for all reservoirs > 0.123 km^3 (100,000 acre feet) in this dataset. There were 258 such structures in RESIS II. We excluded smaller reservoirs due to faster infilling rates and inappropriate representation of sediment accrual in larger reservoirs using data from these smaller water bodies. We then used the *minimum* annual capacity loss rate observed for all reservoirs > 0.123 km^3 in a hydrologic region to estimate the minimum annual storage loss rate for all reservoirs in that hydrologic region (as estimated from the National Inventory of Dams). This minimum rate was extrapolated from the dam closure date forward to either 2010 or 2100, thereby assuming a constant but conservative (minimum observed) infilling rate over the entire forecasting period. Finally, we standardized estimated basin-wide capacity losses by the VIC model estimates of mean annual streamflow such that capacity losses are expressed in terms of the number of years of streamflow lost to dead storage.

The sediment infilling rate (I) and thus, storage loss rate was estimated as above. This infilling rate was converted to a proportion of total storage loss per reservoir (P) by dividing by OC, the original storage capacity (NID Storage):

$$P = \frac{I}{OC}, \text{ in } yr^{-1} \qquad (5)$$

We then used the minimum proportional storage loss rates within a hydrologic basin to represent storage loss for all reservoirs in the same HUC 2 hydrologic unit, or $P_{\min}$, in yr^{-1}. There were no reservoirs larger than 0.123 km^3 in USGS Hydrologic Region 1 from the RESIS II

database, thus we omitted this region from our analysis. Finally, we estimated total losses in the entire hydrologic basin from closure ($t_{closure}$) to 2010 (t_{future}) as:

$$L = P_{\min}\left(t_{future} - t_{closure}\right) * \frac{C_{tot}}{MAF} \quad (6)$$

in yearly equivalents of mean annual streamflow volume where, L is reservoir volume lost *relative* to mean annual streamflow, C_{tot} is total reservoir capacity in the sub-basin (from NID), *MAF* is mean annual streamflow (from the VIC model).

c. Caveats

Our methods for extrapolation include three steps with unique uncertainties. Here we discuss the qualitative magnitude and direction of any biases that these uncertainties may introduce into our estimates of region wide storage losses associated with sediment infilling. The three steps are 1) estimation of infilling rates using RESIS-II data which were often focused on small reservoirs in regions in which sediment loads were high, and for the most part do not include recent (post-1980) measurements, 2) reduction of RESIS-II to a dataset including reservoirs > 0.123 km^3 in storage capacity, 3) extrapolation from the minimum observed infilling rate from a single large reservoir in a hydrologic region to the total capacity losses of all reservoirs in that region. As above, our point estimates of storage loss from dam closure to 2010 for reservoirs in RESIS II assume stationary infilling rates. For example, infilling estimates based on 50 year old sediment surveys have likely changed in response to land use, dam construction in the upstream portions of the watershed and other factors. Similarly, in extrapolating minimum observed infilling rates to all other reservoirs in the same hydrologic subregion, we make the assumption that sediment fluxes and infilling are spatially homogenous at the resolution of hydrologic subregions. Due to these limitations we could potentially overestimate infilling related problems if we had included all reservoirs in the database. This overestimation is not unique to reservoirs west of the 100th Meridian, and hence may not bias our comparison of infilling east and west of this divide. We attempt to compensate for this potential bias by using only large reservoirs in RESIS-II and by using the reservoir in a HUC 2 region with the *minimum* infilling rate as a point of departure for extrapolation and applying this rate uniformly across whole hydrologic regions. Thus, potential overestimates in steps 1 & 2 are potentially offset by applying the most conservative infilling rate during extrapolation in step 3.

6. Firm yield—sequent peak analysis, including forecasted reductions by 2100

a. Data sources

Monthly streamflow – Monthly observed streamflow at select USGS gauging stations was obtained from the National Water Information System (NWIS). Stations were selected with the goal of obtaining up to 20 water years of data, for uncontrolled conditions, for the station with drainage area closest to that of the final reservoir. Monthly streamflow was not available for seven stations for the period of interest, so monthly averages were calculated from the daily observed data.

b. Methods

Firm yield refers to the largest quantity of flow (or withdrawal) that is dependable at a given site along a river system at all times (S30). Firm yield is therefore a function of the active

reservoir storage, and the magnitude and variability of monthly inflows. Firm yield for 24 reservoirs included in the RESIS II database was determined using the sequent-peak method (S30) based on monthly observed streamflow.

Rates of sediment infilling (Section 4) were used to calculate reservoir capacity in 2010 was then calculated as:

$$C_{2010} = C_{closure} - I^*(2010\text{-}Y_{closure}) \quad (7)$$

Where C_{2010} and $C_{closure}$ are the estimated reservoir capacity in 2010 and the actual capacity at closure, respectively. I is the sediment infilling rate in acre-ft/year and $Y_{closure}$ is the year in which reservoir filling began.

Streamflow time series were rescaled by the ratio of the reservoir drainage area to station drainage area, to obtain a best estimate of inflow volume to the reservoir. If sufficient data did not exist for a gauge downstream of the dam for the years before the reservoir was filled, the nearest upstream station(s) were selected. To minimize the influence of climate variability on the firm yield analysis, the closest time interval to the date of dam closure was selected (Table S4). The time period is therefore different for each river, but the analysis provides a best estimate of change in firm yield since dam closure due to sediment infilling alone. The selected period of record for each station (shown in Table S4) was repeated to create a 40 year monthly time sequence, in order to capture the full critical flow sequence if it occurred at the end of the record.

Table S4: USGS gauging sites used in the firm yield analysis of reservoirs

Reservoir	Infilling Date	Drainage area (mi^2)	USGS Sites	Site drainage area (mi^2)	Position nr reservoir	Water Years used
Lake Powell, UT	1963	107700	09380002 Colorado at Lees Ferry	111800	d/s*	1922-1961
Lake Cumberland, KY	1950	5789	03414000 Cumberland River nr Roweena	5790	d/s	1940-1950
Ft Peck Lake, MT	1937	57725	06115200 Missouri River nr Landusky	40987	u/s#	1935-1954
Lake Texoma, OK	1942	33783	07316000 Red R nr Gainsville	30782	u/s	1937-1956
Pine Flat Lake, CA	1952	1542	11218700 Kings River nr Balch Camp	~1342	u/s	1970-1990
John H Kerr Reservoir, VA	1952	7800	02079000 Roanoke at Clarksville	7393	u/s	1936-1952
Elephant Butte Reservoir, NM	1915	25923	08358500 Rio Grande at San Marcial	27700	d/s	1925-1944
Lake Whitney, TX	1951	17656	08091000 Brazos nr Glen Rose	25818	d/s	1942-1961
John Martin Reservoir, CO	1942	18130	07124000 Arkansas at Los Animas	14417	u/s	1975-1994
Fontana Lake, NC	1944	1571	03515000 Little Tennessee at Fontana	1571	d/s	1939-1944
Lake Isabella, CA	1952	2074	11187000 Kern at Isabella	1068	u/s	1926-1935
			11188000 Kern at Kernville	1009	u/s	
Bluestone Lake, WV	1949	4603	03180001 New River at Bluestone	4602	d/s	1939-1949
Glendo Reservoir, WY	1957	19504	06652000 North Platte at Orin	15025	u/s	1959-1978

Lake Mead, NV	1935	167800	09421500 Colorado below Hoover Dam[1]	171700	d/s	1927-1946
Santa Felicia Dam, CA	1955	425	11109600 Piru Creek above Lake Piru	372	u/s	1956-1975
Deer Creek Dam, OH	1968	277	03230800 Deer Ck at Mt Sterling	228	u/s	1967-1981
Gibson Dam, MT	1929	575	06078500 NF Sun R nr Augusta	258	u/s	1946-1965
Ft Supply Dam, OK	1942	1735	07236000 Wolf Cr nr Fargo	1624	u/s	1943-1963
Ocoee No. 1, TN	1911	595	03563000 Ocoee at EMF	524	u/s	1914-1933
Lloyd Shoals Dam, GA	1910	1414	02210500 Ocmulgee R nr Jackson	1420	d/s	1906-1910
Jemez Canyon Dam. NM	1953	1034	08329000 Jemez below Jemez Canyon	1038	d/s	1944-1952
Tionesta Dam, PA	1940	478	030109000 Tionesta R at Nebraska	469	u/s	1924-1940
Angostura Dam, SD	1949	9100	06400500 Cheyenne R nr Hot Springs	8710	u/s	1944-1964
Bartlett Dam, AZ	1939	5812	09510000 Verde R below Bartlett	6161	d/s	1914-1933

*d/s is Downstream and [#]u/s is Upstream

Table S5: Estimated original firm yield and projected firm yield in 2010 for selected 24 reservoirs

Name	Original capacity (km3)	2010 capacity (km3)	%change in capacity	Original Yield (km3/yr)	2010 Yield (km3/yr)	% change in yield
Deer Creek Dam, OH	0.126	0.125	-0.950	0.159	0.158	-0.454
Ft Supply Dam, OK	0.132	0.129	-2.546	0.061	0.060	-0.977
Ocoee No. 1, TN	0.135	0.086	-36.347	0.692	0.579	-16.448
Lloyd Shoals Dam, GA	0.139	0.068	-51.259	1.195	0.982	-17.863
Tionesta Dam, PA	0.165	0.162	-1.792	0.337	0.333	-1.311
Bluestone Lake, WV	0.778	0.754	-3.169	3.081	3.039	-1.373
Fontana Lake, NC	1.795	1.753	-2.337	2.746	2.730	-0.573
Lake Whitney, TX	2.490	2.351	-5.569	0.745	0.734	-1.488
John H Kerr Reservoir, VA	3.464	2.903	-16.201	6.889	6.552	-4.888
Lake Texoma, OK	7.227	5.900	-18.365	2.740	2.601	-5.099
Lake Cumberland, KY	7.511	7.463	-0.637	6.654	6.640	-0.210
Angostura Dam, SD	0.168	0.090	-46.264	0.081	0.059	-27.050
Santa Felicia Dam,CA	0.125	0.108	-13.424	0.042	0.040	-5.337
Gibson Dam, MT	0.129	0.116	-10.268	0.318	0.300	-5.565
Jemez Canyon Dam, NM	0.145	0.108	-25.372	0.043	0.043	-1.970
Bartlett Dam, AZ	0.225	0.211	-6.513	0.365	0.356	-2.415
Lake Isabella, CA	0.703	0.679	-3.414	0.469	0.467	-0.249
John Martin Reservoir, CO	0.866	0.684	-20.992	0.240	0.226	-5.891
Glendo Reservoir, WY	0.983	0.949	-3.493	1.589	1.579	-0.618
Pine Flat Lake, CA	1.250	1.233	-1.382	0.404	0.403	-0.352
Elephant Butte Reservoir, NM	3.250	2.796	-13.969	1.135	1.110	-2.143
Ft Peck Lake, MT	24.124	22.532	-6.599	10.117	9.931	-1.833

Lake Powell, UT	35.550	33.390	-6.076	14.323	14.253	-0.486
Lake Mead, NV	40.052	31.592	-21.122	18.729	18.426	-1.618

c. Method documentation

The sequent peak algorithm (SPA) (S31), the equation form of a graphical approach first proposed by Rippl (S32), is a well-known approach for reservoir storage analysis based on a mass balance equation to determine required storage to prevent any shortfalls during a critical period of river inflows. It is documented in basic engineering text books (e.g. (S30) and is still used in modern research (e.g.(S33, 34). McMahon et al. (S34) implemented SPA in a similar manner to our application, to examine the relationship between storage requirements and flow variation for global rivers. The primary difference is that McMahon et al. (S34) used a fixed record length of 25 years, while our record length varied from four to 40 years depending on flow availability. Adeloye (S33) has shown that a short record length will produce a negative bias in estimates of reservoir reliability and storage capacity, which reduces with increasing record length.

d. Caveats

Firm yield estimates are based on the assumption of constant infilling rates and estimated storage losses over time (see caveats in Section 5). Infilling in reservoirs in our firm yield analysis may have slowed due to closure of new dams upstream. The sequent peak analysis assumes that the time interval includes the critical period which will result in the greatest drawdown of reservoir levels. Where sediment loads delivered to the reservoirs in our analyses have slowed either because of climate, land use or closure of dams upstream, we may overestimate firm yield losses.

7. Estimating revenue losses due to saline soils

a. Data sources

The most recent available data for soil salinity, crop salt tolerances, crop yields, prices and distributions were used at the time of analysis (October 2009). Data sources are summarized in Table S6.

Table S6: Data sources for estimating revenue losses due to saline soils

Data	Source	Spatial resolution	Time period (Year)
Soil salinity	USDA-NRCS [1]	Variable (STATSGO soil mapping units)	2006
Crop salt tolerance	FAO [2]	N/A	N/A
Crop types	USDA-NASS [3]	56 m	2008 (if missing: 2007 or 2001)
Crop yields	USDA-NASS [4]	County or State	2008
Crop prices	USDA-NASS [4]	State	2008

[1] http://soildatamart.nrcs.usda.gov
[2] http://www.fao.org/docrep/005/Y4263E/y4263e0e.htm
[3] http://www.nass.usda.gov/research/Cropland/SARS1a.htm and http://datagateway.nrcs.usda.gov/
[4] http://www.nass.usda.gov/Data_and_Statistics/Quick_Stats/index.asp

b. Methods

The impact of saline soils on agricultural revenues was estimated based on a commonly used, empirically determined relation between soil salinity and relative crop yield (S35),

$$Y_r = 1 - \frac{b\left(EC_e - a\right)}{100} \qquad EC_e > a$$
$$Y_r = 1 \qquad EC_e \le a \tag{12}$$

where Y_r is relative crop yield [-], defined as the ratio between actual (salt-affected) crop yield Y_a and potential crop yield Y_p in the absence of soil salinity, EC_e is soil salinity, expressed as electrical conductivity of a soil saturated paste extract [dS/m], and *a* [dS/m] and *b* [% yield reduction per dS/m] are crop-specific salt tolerance parameters, describing the reduction in crop yield as soil salinity increases. The model in Eq. (12) has been used in many studies (e.g., (S36-39), and representative values of *a* and *b* have been experimentally determined for a large number of crops (S35, 40) and references therein).

Relative crop yield Y_r from Eq. (12) was converted into a corresponding crop yield loss Y_L [yield unit/acre], using the definition of relative crop yield,

$$Y_L = Y_p - Y_a = Y_p\left(1 - Y_r\right) = Y_a \frac{1 - Y_r}{Y_r} \tag{13}$$

Next, these yield losses Y_L were converted into salinity related revenue losses R_L [USD/acre],

$$R_L = P_c Y_L \tag{14}$$

where P_c is crop price [USD/yield unit]. Note that revenue loss is computed here relative to a situation without salinity.

To account for the spatial variation in soil salinity, crop yields, crop prices, and crop types, Eq. (14) was applied on a horizontal grid with a resolution of 0.008333 degrees in both longitudinal and latitudinal directions, so that each grid cell represents a unique combination of soil salinity, crop yield, crop price, and crop type. Cell areas on this grid vary in size between 130 and 190 acres, with an average of 160 acres (approximately 800 m by 800 m). For each grid cell, crop revenue losses were estimated using Eq. (14), and the resulting values were subsequently summed over each HUC-4 area, i.e.,

$$R_{L,HUC-4} = 10^{-6} \sum_i \left(R_L A\right)_i \tag{15}$$

where *A* is grid cell area [acres], and HUC-4 revenue losses $R_{L,HUC-4}$ are expressed in million USD (hence, multiplication by a factor of 10^{-6}), as in Figure 3C.

Processing steps that were used to arrive at the results in Figure 3C were as follows.

- Soil salinity: Soil salinity estimates were obtained from the STATSGO soil map of the conterminous US. First, depth-averaged soil salinity was computed for each component of each soil mapping unit, followed by weighted-averaging (with weights proportional to relative areas of soil map components) to obtain average soil salinity for each mapping unit. This resulted in representative values for soil salinity for each soil mapping unit.
- Crop salt tolerance: Crop-specific salt tolerance parameters *a* and *b* in Eq. (12) were obtained from previous studies, as summarized in Tanji and Kielen (S40). A total of 67 crops were considered here, including all major crops grown in the US and a range of smaller crops as well.
- Crop types: Spatially distributed crop classification maps, available by state as Crop Data Layers (CDL) from the USDA National Agricultural Statistics Service (NASS), were compiled into a national crop type map. These maps were originally derived from

satellite imagery at a spatial resolution of 56 m, as discussed in more detail in the html reference in Table S6. The most recent crop classification maps were used. For most states, this corresponds to the year 2008. Exceptions are California (2007), Oregon (2007), Washington (2007), Montana (2007), Idaho (2007), Florida (2004), Connecticut (2002), and Rhode Island (2002). For the following states, no crop classification maps were available, and more general land use data from the 2001 National Land Cover Dataset (NLCD) were used instead: Massachussetts, Maine, New Hampshire, New Mexico, Vermont. For these five states, areas mapped as cropland were assumed to be planted with the state's dominant crop type (typically, hay). All state maps were resampled to the 0.008333-degree grid used in this study, and were spatially merged to create a national crop classification map.

- Crop yields and prices: Data on crop yields and crop prices for the year 2008 were obtained from the USDA NASS. Crop prices are typically available at state level, whereas yield data are reported by county for all major crops, except vegetables, fruit, and nuts, which are reported by state.

c. Caveats

Limitations of our analysis are related to data accuracy, and to the spatial and temporal variability of the variables of interest, i.e. soil salinity, crop salt tolerance, crop types, yields, and prices.

- Data accuracy: Soil salinity values from the STATSGO database should be considered indicative, as they are based on a combination of field and lab measurements, and best judgment by soil scientists performing the survey. Yield losses in areas without reported salinity values were assumed to be negligible, as such areas typically coincide with wet climates (e.g., parts of the eastern U.S.). Accuracy of the crop maps varies with crop type, and is typically greater for common crops, such as corn and soybean, than for small crops, such as vegetables. Details on crop classification accuracies are available via the link provided in Table S6. A fraction (35%) of the area classified as "hay/pasture" was assumed to be harvested as hay in 2008, in order to achieve a good match with reported acreages for hay crops (Table S7). Salt tolerance parameters used in Eq. (12) were obtained from literature, and should be considered indicative, as salinity effects may vary with local field conditions.
- Spatial variability: Another limitation is that the data listed in Table S6 are not all available at the same high spatial resolution. Crop type maps have the largest resolution ("field-scale"), whereas crop yields are only available at either county or state level. This means that actual recorded crop yields are averages over an area that in general includes both salt-affected and non-affected regions. To account for the effects of spatial heterogeneity at the county and state level, crop revenue losses in Eq. (13) were computed assuming that reported crop yields are representative for either saline or non-saline conditions. This results in two separate estimates for Y_L in Eq. (13): one assuming that Y_a equals reported yield, and the other assuming that Y_p equals reported yield. Results in Figure 3C show the average of these two estimates. A further implication of limited spatial resolution is the occasional occurrence of very high yield reductions in Eq. (12), e.g. when a salt-sensitive crop coincides with a highly saline grid cell; here we assumed that yield reductions were at most 50%.

- Temporal variability: A limitation of our estimates is that they are static, in the sense that they ignore any temporal variations in salinity, crop types, yields, and prices. In reality, farmers may adapt to changing soil, agronomic, and economic conditions by adjusting their cropping and irrigation practices, e.g. switching from high-valued, salt sensitive crops to low-valued, salt tolerant crops. This provides a level of flexibility and adaptation that may alleviate negative impacts of soil salinity. However, the degree of adaptation will be determined by local and regional economic, technological, social, and resource constraints. A careful assessment of all these factors at the national scale is beyond the scope of this study.

d. Validity and robustness of results

In view of the limitations discussed above, the results obtained in this study (Fig. 3C) should be treated as order of magnitude estimates based on the most recent and best available data at the national scale.

Table S7: Estimated and actual harvested crop acreages for 2008 (in million acres)

Crop category	Estimated	Harvested
Corn	79.4	78.6
Soybeans	71.3	74.7
Wheat and other grains	65.5	68.9
Hay	58.3	60.1
Other field crops	21.3	22.7
Vegetables	1.5	2.9
Fruit and nuts	3.1	3.6
TOTAL	**300.3**	**311.6**

As estimated revenue losses are based on crop maps derived from remote sensing data (see data sources above), it is useful to compare estimated crop acreages from the crop maps with aggregated national crop statistics from the USDA-NASS. Table S6 shows such a comparison for 7 major crop categories. At this aggregated scale, the numbers compare quite well, with the exception of vegetable crops, where the relative error is quite large - this crop category consists of a wide array of different vegetables, each with fairly small acreages, making identification via remote sensing difficult. As noted above, the match for harvested hay acreages includes a partial crop map reclassification from “hay/pasture” to harvested hay.

In terms of revenue losses, the spatial patterns in Fig. 3C highlight areas commonly associated with salinity problems in agriculture, namely the San Joaquin Valley in California, the southern part of the Colorado basin, the Upper Snake basin, and the northern Great Plains. Total annual revenue loss due to salinity amounts to 2.8 billion USD, or approximately 2% of total crop revenue in 2008. In salt-affected areas, this number increases regionally to 10% and locally to 50%.

Sensitivity of estimated revenue losses to spatial variability of soil salinity at county and state levels was relatively small: assuming reported crop yields to be representative of either non-saline or saline conditions (see above), total estimated revenue losses were 2.1 and 3.5 billion USD, respectively, with an average of 2.8 billion USD. Other uncertainties related to data accuracy and temporal variability, as discussed above, may further increase this range. To assess sensitivity of our results to STATSGO soil salinity values, we also computed losses assuming

that soil salinity is limited anywhere to a maximum value of 4 dS/m. This assumption corresponds to the lowest salinity estimates for a fixed saline soil extent (since soil is considered saline if EC_e > 4 dS/m), thereby establishing a reasonable lower bound on losses. For this scenario, revenue losses ranged between 1.4 and 1.9 billion USD, with an average of 1.7 billion USD. Finally, in view of the results in Table S7, an under-estimation of the actual harvested acreage of vegetable crops, which are typically high-valued and salt-sensitive, suggests that our estimates are somewhat conservative in this respect.

As partial verification of our results, we consider the work of Howitt et al. (S41), which investigated the economic costs of increased salinity in California's Central Valley. For an increase of 13% in salt-affected agricultural land by the year 2030, Howitt et al. (S41) estimated a corresponding increase in annual revenue loss of 185 million USD (in 2008 dollars). Scaling up this estimate to the current salt-affected extent (i.e., 100% or multiplying by a factor of 7.7), amounts to annual revenue losses of 1.4 billion USD – this corresponds well with our total loss estimate of 1.3 billion USD for the HUC-4 regions located in the Central Valley of California. However, care should be taken in comparing these two numbers, as one is based on changes in revenue loss using agro-economic optimization under assumed changes in crop demand and prices by 2030 (S41), whereas the other estimates current losses using data from 2006-2008.

8. Biodiversity—The proportion of non-native fishes and the prevalence of non-native predators

a. Data sources

We used the USGS Non-indigenous Aquatic Species (NAS) and NatureServe's Distribution of Native U.S. Fishes by Watershed datasets to quantify absolute numbers of native and non-native fishes and the ratio of non-natives to natives in each USGS hydrologic subregion (HUC 4 basin). Both datasets consist of literature based occurrences (presence/absence data) in each HUC 8 accounting unit.

b. Methods

We summed unique species across all accounting units (8-digit hydrologic units) within a subregion (4-digit hydrologic units) using common names. We used common names rather than scientific names available in these databases to exclude subspecies and avoid overestimation of native and non-native richness. For non-native species we used only those classified as established or stocked. Finally, we quantified the prevalence of non-native species based on the proportion of 8-digit accounting units in which each species was observed across the coterminous US. The top 25 most prevalent of these species (presence in highest proportion of HUC-8 basins in Regions 13-18) were then classified in terms of their origin (from subregions east of the 100th Meridian and inhabiting slow lotic or lentic habitats), capacity for piscivory (eats other fish or not), and capacity for eating other non-native piscivores (e.g., a smallmouth bass eats bluegill as well as a native cyprinid). Classifications for the top 25 most prevalent non-native fishes are shown in Table S2 (above).

c. Caveats

NAS and Natureserve data are binary (presence/absence) data. As such, patterns reported reflect the distribution not abundance of either group of species.

9. Virtual water footprint estimation

a. Data sources

Metropolitan Statistical Areas (MSA): We identified all MSAs defined by the United States Office for Management and Budget (OMB) with 2000 census population in excess of 100,000. The OMB defines a Metropolitan Statistical Area as all areas adjacent to an urban core that have a high degree of social and economic integration with the urban core. MSA populations were obtained from the U.S. Census Bureau, and the representative MSA latitude and longitude were downloaded from the ZIP Code Download digital database.

Nutritional Water Use (NWU): Renault and Wallender (S42) estimated the total nutritional water use (NWU) needed to produce food for a typical US diet to be 5.4 m^3 per capita per day.

b. Methods

In a regional budget of virtual water (VW) embedded in food production net VW import ($VW_{imported}$ - $VW_{exported}$) is balanced by the VW produced in the region via food crop production ($VW_{produced}$) and the VW consumed by the population in the region ($VW_{consumed}$), such that:

$$\Delta VW = (VW_{imported} - VW_{exported}) = (VW_{consumed} - VW_{produced}) \quad (16)$$

The VW consumed for each MSA, in cubic meters per year, was estimated as NWU times the MSA population, assuming that, on average, all individuals have a NWU equal to that of the typical US diet. The VW produced is based on the crop water use for irrigated and rainfed crops grown in the region, as well as water used for animal production. $VW_{produced}$ was calculated on a per capita basis for the HUC 4 corresponding to each MSA, as the sum of total water withdrawals for irrigation, livestock and aquaculture (from the USGS Water Use data, Section 3) and estimated crop water use due to rainfall alone. Rainfed crop water use was estimated using HUC 4 average actual evapotranspiration estimates from the VIC model (Section 1), times the cropped area of the HUC. The total area in food crops in each HUC 4 was calculated using the USDA-NASS crop type layer (Section 7) using the 87 categories that correspond to human or animal food products.

The net VW import volume is converted to an equivalent footprint area, by dividing by the average depth of streamflow (total runoff) estimated from the VIC model (Section 1) from the corresponding HUC 4.

c. Method documentation

The concept of a water footprint, independent from the overall ecological footprint, was explored by Hoekstra and Chapagain (S43, 44). They define the water footprint at the national scale to represent the "volume of water needed for the production of the goods and services consumed by inhabitants of the country" (S44). They define an internal water footprint as the total water volume used from domestic water resources in the national economy minus the exported volume (VWproduced – VWexport) and an external footprint composed of virtual water import minus the re-export of imported products (VWimport – VWre-export). For our analysis, we only include the virtual water imbedded in food production and consumption, excuding the virtual water of domestic use and industrial products. In addition, there are two major innovations in our approach: 1) we moved to the sub-national scale to calculate the net virtual water flows for individual metropolitan areas (VWimport – VWexport) and 2) we normalize the water volumes by average annual runoff depth, to convert to an equivalent land area, in keeping with the

original concept of "Ecological Footprints". Our estimates of agricultural water use are consistent with those outlined by Hoekstra and Chapagain (S44). Rather than using data on trade flows to directly estimate import and export however, we use assumptions about local consumption of virtual water, through published data on typical US diets.

d. Caveats

As in Section 3, the water use dataset we use reflects the location of water withdrawals, rather than the destination of extracted water (to the user). Water transfers from upstream reservoir storage to croplands lower in the basin, for example will create distortions in the distribution of water withdrawals. As such net positive virtual water footprints in some cities (e.g., Havasu City, AZ and Colorado Springs, CO) may reflect agricultural production and export in distant portions of the same subregion or a neighboring subregion. The magnitude of the net virtual water footprint is not biased by this small spatial imprecision.

10. Estimating WSI and virtual WSI for the Cadillac Desert super-region

a. Data sources & methods

For the analyses in Figure 4b, we define the Cadillac Desert super-region as the land area represented by USGS Hydrologic Regions (2-digit hydrologic unit codes): 14-17 and 18, as well as subregions 1019 and 1102. This super-region includes the Rio Grande, Upper and Lower Colorado, Great Basin and California hydrologic regions as well as the front range headwaters of the South Platte and Arkansas River drainages.

Actual water scarcity—We estimate *WSI* as the ratio of total water withdrawals to mean annual streamflow $WSI = W/MAF$ as in Figure 3a in the main body. Below we describe how we compiled data for the more regional estimates of *W*, *MAF* and *WSI* included in Figure 4b. As in Figure 3b, withdrawals include surface and groundwater, as this best represents total demand for freshwater resources. We then compare this to the streamflow generated within the subregion to gage the capacity for renewable freshwater resources (surface water) to provide adequate supply for this demand.

Withdrawals, W—Here we estimate *W* within each USGS subregion as in Section 2. We then sum *W* across HUC4s within Hydrologic Regions 13,14,15,16 and 18. We also include *W* for front-range population centers in Colorado (Hydrologic Regions 10 and 11) by adding *W* for subregions 1019 and 1102 to Region 14. We add subregions 1019 and 1102 to region 14 because the cities in subregions 1019 and 1102 depend on trans-continental divide diversions of surface water from the headwaters of the Colorado River in region 14.

Streamflow, MAF—We computed a sum of estimated mean annual streamflow (from the VIC model) generated within each of the Hydrologic Regions (13-16 and 18) and within each of the subregions from the front range of Colorado (subregions 1019 and 1102). In this regional estimation of WSI, we ignore flow routing in our estimate of *MAF* as we are summing across entire basins or using only the most upstream subregions (1019 and 1102).

WSI—The water scarcity index for the entire super-region can be estimated as $WSI = \sum W / \sum MAF$, where $\sum W$ and $\sum MAF$ are sums across hydrologic regions 13-17 & 18 and subregions 1019 and 1102.

Virtual water scarcity: We define virtual water scarcity as $WSI' = \sum W' / \sum MAF$, where $W' = W_{M\&I} + W_{virtual}$, $W_{M\&I}$ is actual municipal and industrial (M&I) withdrawals, $W_{vritual}$ is the *virtual* water needed for agriculture, and *MAF* is defined in the previous section as mean annual streamflow. As above $\sum W'$ and $\sum MAF$ are sums across hydrologic regions 13-17 & 18 and subregions 1019 and 1102. Actual M&I withdrawals are identical to those used in the calculation of actual *WSI* for the super-region. They include public supply, domestic self-supply, industrial, mining and thermoelectric power self-supply withdrawals in 2000 as in Figure 3a (Section 2 above). Total annual virtual water is estimated as $W_{virtual} = g * Pop$. Here *g*, is the per capita annual water volume required to grow the average US diet (or, 5.4 $m^3*day^{-1}*person^{-1}$ x 365 $days*yr^{-1}$ = 1971 $m^3*yr^{-1}*person^{-1}$) and *Pop* is the population of the hydrologic region or subregion. Population estimates by subregion were estimated from county level Census 2000 data. Thus virtual *WSI* differs from actual *WSI* only in the way we account for agricultural water. In actual *WSI*, agricultural withdrawals reflect actual water extracted within the super-region to support agriculture. In virtual *WSI*, agricultural withdrawals reflect all water indirectly consumed by people in the super-region via the production of food. In this way, virtual *WSI* also gives an index of the theoretical water withdrawals that would be needed to grow all food locally (within the super-region) via irrigation by diverted streamflow.

b. Caveats

We note here that the VIC model underestimates streamflow in the Colorado River basin (Table S3), a key watershed in our analysis of water scarcity in the Cadillac Desert super-region (Figure 4b). In particular, our model evaluation exercise suggests that we underestimate streamflow at Imperial Dam (~74% of the entire Colorado River drainage area) by -6.8% (a volume of 1.45 km^3 per year). We correct for this bias by using naturalized streamflow data for the portion of the Colorado River basin above Imperial Dam. Thus, MAF for the region is tallied as above, but replacing the VIC model simulated streamflow from grid cells above Imperial Dam with real data (mean annual naturalized streamflow). This correction decreases our estimate of WSI for the super-region by only ~ 1%.

11. Estimating water use, WSI and virtual WSI under a population doubling scenario

a. Data sources & methods

To estimate *WSI* and WSI' under a population doubling scenario, we projected total *future* water withdrawals (W_f and W_f', respectively) using USGS population and water use data (http://water.usgs.gov/watuse/) assuming a doubling of the entire population of the Cadillac Desert super-region.

The USGS has catalogued total water withdrawals every five years since 1950 for the entire US. These data are coupled with census estimates of the US population. Water use closely tracked population growth from 1950-1980, but flattened out (shallower increase in water use with population growth) from 1985-2005. Recent trends indicate significant improvements in water use efficiency—water withdrawals have increased much more modestly since the publication of Cadillac Desert than prior to this book.

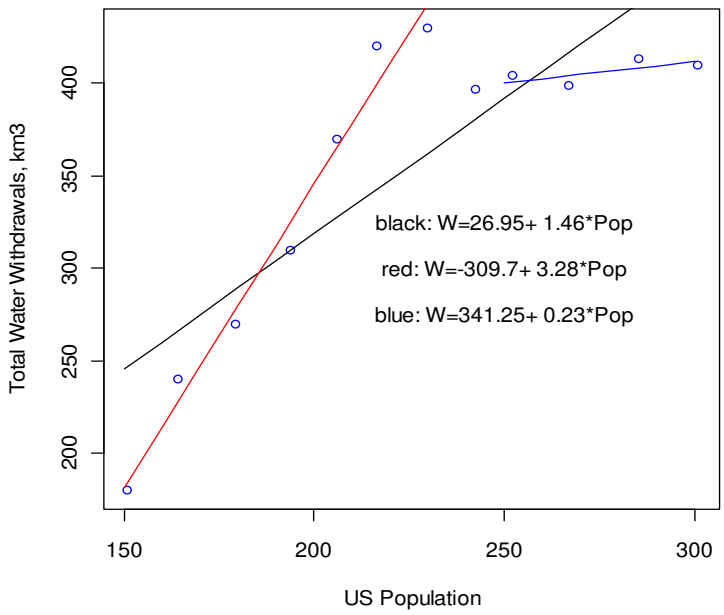

Figure S5: Regression relationships between US population (in millions) and water use (total freshwater withdrawals).

To project total water withdrawals we developed a series of regression relationships between population and total water withdrawals:

- Using all available data (1950-2005)
- Using data up until the writing of Cadillac Desert (1950-1980)
- Using data from the publication of Cadillac Desert to present (1985-2005), 2010 data are not yet available. Note that water use data do not become available immediately.

To project WSI and WSI' we used the slope of the regression relationship between population and water use only for the most recent data (e.g., 1985-2005, or a slope = 0.23) to project water withdrawals assuming a doubling in population size (Figure S5, blue line). Projected withdrawals (W_f and W_f') are estimated as $W_f = W + 0.23 * \Delta Pop$ and $W_f' = W' + 0.23 * \Delta Pop$, respectively, and ΔPop is the change in population size (or, $2Pop - Pop = Pop$). The actual and virtual water scarcity indices were then estimated the entire super-region under a population doubling scenario as $WSI_{future} = \sum W / \sum MAF$ and $WSI'_{future} = \sum W' / \sum MAF$, respectively, where $\sum W$, $\sum W'$ and $\sum MAF$ are sums across hydrologic regions 13-17 & 18 and subregions 1019 and 1102.

b. Caveats

Our forecast of WSI and WSI' under a population doubling scenario relies on the assumption that the current relationship between population growth and water use (low slope) will prevail over the next century and that population growth will continue at current rates such that census bureau projections for 2030 are realized and the rates used for these projections prevail over the next 50-90 years. If population growth in the Cadillac Desert slows and/or water use efficiency increases to the extent that the slope between water use and population size declines even further than it has since the publication of the book Cadillac Desert, then we will overestimate future levels of water scarcity.

References

S1. Cherkauer K & Lettenmaier D (1999) Hydrologic effects of frozen soils in the Upper Mississippi River basin. *J. Geophys. Res.* 104(D16):19599-19610.

S2. Liang X, Lettenmaier D, Wood E, & Burges S (1994) A simple hydrologically based model of land surface water and energy fluxes for general circulation models. *J. Geophys. Res.* 99:14415-14428.

S3. Liang X, Lettenmaier D, & Wood E (1996) One-dimensional statistical dynamic representation of sub-grid spatial variability of precipitation in the two layer variable infiltration capacity model. *J. Geophys. Res.* 101:21403-21422.

S4. Maurer E, Wood A, Adam J, Lettenmaier D, & Nijssen B (2002) A long-term hydrologically based dataset of land surface fluxes and states for the conterminous Unites States. *J. Clim.* 15:3237-3251.

S5. Lohmann D, Raschke E, Nijssen B, & Lettenmaier D (1998) Regional scale hydrology: I. Formulation of the VIC-2L model coupled to a routing model. *Hydrological Sciences Journal* 43:131-142.

S6. Lohmann D, Raschke E, Nijssen B, & Lettenmaier D (1998) Regional scale hydrology: II. Application of the VIC-2L model to the Weser River, Germany. *Hydrological Sciences Journal* 43:143-158.

S7. Adam J, Hamlet A, & Lettenmaier D (2009) Implications of global climate change for snowmelt hydrology in the 21st century. *Hydrological Processes* 23(7):962-972.

S8. Bowling L, et al. (2003) Simulation of high-latitude hydrological processes in the Torne-Kalix basin: PILPS Phase 2(e) 1: Experiment description and summary intercomparisons. *Global and Planetary Change* 38:1-30.

S9. Bowling L, et al. (2003) Simulation of high-latitude hydrological processes in the Torne-Kalix basin: PILPS Phase 2(e) 3: Equivalent model representation and sensitivity experiments. *Global and Planetary Change* 38:55-71.

S10. Cherkauer K & Lettenmaier D (2003) Simulation of spatial variability in snow and frozen soil. *J. Geophys. Res.* 108(D22):19-11 to 19-14.

S11. Christensen N & Lettenmaier D (2006) A multimodel ensemble approach to assessment of climate change impacts on the hydrology and water resources of the Colorado River basin. *Hydrol. Earth Syst. Sci. Discuss.* 3:3727-3770.

S12. Christensen N, Wood A, Voisin N, Lettenmaier D, & Palmer R (2004) The effects of climate change on the hydrology and water resources of the Colorado River Basin. *Clim. Change* 62:337-363.

S13. Hamlet A, Mote P, Clark M, & Lettenmaier D (2007) 20th Century Trends in Runoff, Evapotranspiration, and Soil Moisture in the Western U.S. *J. Climate* 20(8):1468-1486.

S14. Mitchell K (2004) The multi-institution North American Land Data Assimilation System (NLDAS): Utilizing multiple GCIP products and partners in a continental distributed hydrologic modeling system. *J. Geophys. Res.* 109:1-32.

S15. Nijssen B, O'Donnell G, Lettenmaier D, Lohmann D, & Wood E (2001) Predicting the discharge of global rivers. *J. Clim.* 14:3307-3323.

S16. Nijssen B, Schnur R, & Lettenmaier D (2001) Global retrospective estimation of soil moisture using the variable infiltration capacity land surface model, 1980-93. *J. Clim.* 14:1790-1808.

S17. Wood E, Lettenmaier D, Liang X, Nijssen B, & Wetzel S (1997) Hydrologic modeling of continental-scale basins. *Annu. Rev. Earth Planet. Sci.* 25:279-300.
S18. Abdulla F, Lettenmaier D, & Liang X (1999) Estimation of the ARNO model baseflow parameters using daily streamflow data. *J. Hydrol.* 222:37-54.
S19. Miller D & White R (1998) A conterminous United States multilayer soil characteristics dataset for regional climate and hydrology modeling. *Earth Interactions* 2:1-26.
S20. Nash J & Sutcliffe J (1970) River flow forecasting through conceptual models part I - A discussion of principles. *J. Hydrol.* 10:282-290.
S21. Bowling L & Lettenmaier D (2010) Modeling the Effects of Lakes and Wetlands on the Water Balance of Arctic Environments. *J. Hydrometeorol.* 11:276-295.
S22. Sinha T & Cherkauer K (2010) Impacts of future climate change on soil frost in the midwestern United States. *J. Geophys. Res.* 115(D08105):16 p.
S23. Su F, Adam J, Trenberth K, & Lettenmaier D (2006) Evaluation of surface water fluxes of the pan-Arctic land region with a land surface model and ERA-40 reanalysis. *J. Geophys. Res.* 111(D05110):doi:10.1029/2005JD006387.
S24. Huson S, et al. (2005) Estimated Use of Water in the United States in 2000 (U.S. Geological Surve Circular 1268, Denver, CO), p 52 p.
S25. Kenny J, et al. (2009) Estimated Use of Water in the United States in 2005. (U.S. Geological Survey Circular 1344), p 53 p.
S26. Ackerman K, et al (2009) RESIS–II—An updated version of the original reservoir sedimentation survey information system (RESIS) database. (U.S. Geological Survey Data Series 434, available at http://pubs.usgs.gov/ds/ds434/).
S27. Zhou X-H & Gao S (1997) Confidence intervals for the log-normal mean. *Statistics in Medicine* 16:783-790.
S28. Gray J, Bernard J, Schwarz G, Stewart D, & KT R (2009) Online Interactive U.S. Reservoir Sedimentation Survey Database. *Eos Trans. AGU* 90(23):doi:10.1029/2009EO230003.
S29. Graf W, Wohl E, Sinha T, & Sabo J (in press) Sedimentation and Sustainability of Western American Reservoirs. *Water Resour. Res.*:doi:10.1029/2009WR008836.
S30. Mays L & Tung Y (1992) *Hydrosystems engineering and management* (McGraw-Hill, New York).
S31. Thomas H, Jr & Burden R (1963) Operations research in water quality management. (Harvard Water Resources Group, Cambridge, USA, Massachusetts), pp 1-17.
S32. Rippl W (1983) The capacity of storage reservoirs for water supply. *Minutes of Proceedings, Institution of Civil Engineers*, pp 270-278.
S33. Adeloye A (1990) Streamflow data and surface water resource assessment: a quantitative demonstration of the need for adequate investment in data collection in developing countries. *J. Wat. Supply Res. Tec. (Aqua)* 39(4):225-236.
S34. McMahon T, Vogel R, Pegram G, Peel M, & Etkin D (2007) Global streamflows – Part 2: reservoir storage–yield performance. *J. Hydrol.* 347(3-4):260-271.
S35. Maas E (1990) Crop salt tolerance, In: Agricultural salinity assessment and management. in *ASCE Manuals and Reports on Engineering Practice No. 71*, ed (Ed.) TK.
S36. Cai X, McKinney D, & Lasdon L (2003) Integrated Hydrologic-Agronomic-Economic Model for River Basin Management, J. Water Resources Planning and Management. 129(1):4-17.

S37. Kandil H, Skaggs R, Dayem S, & Aiad Y (1995) DRAINMOD-S: Water management model for irrigated arid lands, crop yield and applications. *Irrigation and Drainage Systems* 3:239-258.
S38. Lefkoff L & Gorelick S (1990) Simulating physical processes and economic behavior in saline irrigated agriculture: model development. *Water Resour. Res.* 26(7):1359-1369.
S39. Letey J & Dinar A (1986) Simulated crop water production functions for several crops when irrigated with saline waters. *Hilgardia* 54:1-32.
S40. Tanji K & Kielen N (2002) Agricultural Drainage Water Management in Arid and Semi-Arid Areas. *FAO Irrigation and Drainage Papers No. 61*:202 p.
S41. Howitt R, et al. (2009) The economic impacts of Central Valley Salinity. in *Final report to the State Water Resources Control Board Contract 05-417-150-0* (Univeristy of California Davis).
S42. Renault S & Wallender W (2000) Nutritional water productivity and diets. *Agricultural Water Management* 45:275-296.
S43. Chapagain A & Hoekstra A (2004) Water footprints of nations'. in *Value of Water Research Report Series No. 16* (UNESCO-IHE, Delft, the Netherlands).
S44. Hoekstra A & Chapagain A (2007) Water footprints of nations: Water use by people as a function of their consumption pattern. *Water Resour. Manage* 21:35-48.